



MARMARA UNIVERSITY
INSTITUTE FOR GRADUATE STUDIES
IN PURE AND APPLIED SCIENCES



**AN EXPERIMENTAL INVESTIGATION OF
WALL EFFECTS IN LIQUID-SOLID
FLUIDIZATION**

ÖZLEM KAPLAN

MASTER THESIS

Department of Environmental Engineering

Thesis Supervisor

Prof. Dr. Ömer AKGİRAY

ISTANBUL, 2017



MARMARA UNIVERSITY
INSTITUTE FOR GRADUATE STUDIES
IN PURE AND APPLIED SCIENCES



**AN EXPERIMENTAL INVESTIGATION OF
WALL EFFECTS IN LIQUID-SOLID
FLUIDIZATION**

ÖZLEM KAPLAN

524314010

MASTER THESIS

Department of Environmental Engineering

Thesis Supervisor

Prof. Dr. Ömer AKGİRAY

ISTANBUL, 2017

ACKNOWLEDGEMENT

First of all, I would like to give my sincere thanks to my advisor Prof. Dr. Ömer Akgiray for giving me the opportunity to take part in this pioneering work, sharing his deep knowledge and making communication possible at all the time. It was possible to start my master study thanks to him. I am grateful to Assist. Prof. Dr. Elif Soyer who always standing with me and encouraging me. I will always follow her patience and hardworking all through my life. I would also like to thank Dr. Selda Yiğit Huncce for everything she taught me. She enlightened me on every issue I have a problem. Working with them is the most valuable experience I have ever had.

I must express my very profound gratitude to my parents, to my sister Rabia and to my boyfriend Hulki Şengür and his family for their love, faith, providing me with unfailing support and continuous encouragement throughout my years of study and through the process of researching and writing this thesis. This accomplishment would not have been possible without them.

I would like to thank instructors and my friends in Marmara University Environmental Engineering Laboratory for their help and support.

This study is supported by the Marmara University Scientific Research Committee (BAPKO; project number FEN-E-130313-0076). This funding is also greatly acknowledged.

June, 2017

Özlem Kaplan

TABLE OF CONTENTS

ACKNOWLEDGEMENT	i
ABSTRACT	iii
SYMBOLS	v
ABBREVIATIONS	vii
LIST OF FIGURES	viii
LIST OF TABLES	ix
1 INTRODUCTION	1
1.1 Characterization of Filter Media	2
1.1.1 Particle density	2
1.1.2 Particle size	3
1.1.3 Particle shape	3
1.2 Fluidization of spherical particles	3
1.3 Wall effects in liquid-solid fluidization	7
2 MATERIALS AND METHOD	13
2.1 Experimental Setup	13
2.2 Materials	19
2.3 Characterization of Materials	21
2.3.1 Particle size	21
2.3.2 Density determination of materials	22
3 RESULTS AND DISCUSSION	26
3.1 Particle Characterization Results	26
3.2 Results of Fluidization Experiments	28
4 CONCLUSIONS	39
REFERENCES	41
ÖZGEÇMİŞ	53

ABSTRACT

AN EXPERIMENTAL INVESTIGATION OF WALL EFFECTS IN LIQUID-SOLID FLUIDIZATION

Fluidized bed expansion correlations developed to date have been based on laboratory scale columns. Wall effects possibly present in small columns, however, may limit the applicability of the resulting correlations to large full-scale equipment in which wall effects are not present. Unfortunately, a systematic evaluation of wall effects is still lacking in the fluidization literature.

Fluidization experiments were carried out in this work using five columns with different diameters and a twenty three different spherical solid media with varying sizes and densities. Characterization of particles was accomplished before the fluidization experiments. Water was used as fluidizing liquid. An important point in this study was that water temperature was aimed to keep at 20 °C by the help of a recirculating chiller/heater bath. Data obtained from experiments was evaluated using some correlations in the literature. These equations are Akgiray and Soyer (2006), Richardson and Zaki (1954), Khan and Richardson (1990), Garside and Al-Dibouni (1977) and Hashizume and Matsue (1998).

Five columns and twenty three different particle types resulted in 115 possible fluidization experiments. Only one of these experiments (10 mm glass balls in the 1 cm column) was not attempted as these balls would touch the walls of the column from all directions and remain motionless due to the resulting physical restriction. Homogeneous fluidization was not possible for $d/D > 0.33$ and was achieved only by vigorous tapping for $0.25 < d/D < 0.33$. The effect of column size on bed expansion was significant in the smallest column in which homogeneous fluidization was possible for the given particle size. Wall effect on bed expansion was observed to be significant for $d/D > 0.2$, whereas slight effects were observed for $0.11 < d/D < 0.2$, and the effect on bed expansion was negligible for $d/D < 0.11$. With more than 4000 separate measurements, the present study is believed to be the most systematic and comprehensive single study focusing on wall effects in liquid-solid fluidization.

June, 2017

Özlem Kaplan

ÖZET

SIVI-KATI AKIŞKANLAŞMASINDA DUVAR ETKİSİNİN DENEYSEL OLARAK ARAŞTIRILMASI

Akışkan yatak genişlemeleri için literatürde kullanılan korelasyonlar laboratuvar ölçekli kolonlara dayanmaktadır. Ancak, küçük kolonlarda bulunan duvar etkisi, bu korelasyonların, duvar etkisinin bulunmadığı büyük ölçekli ekipmanlara uygulanabilirliğini kısıtlamaktadır. Maalesef, akışkanlaşma literatüründe, duvar etkisinin sistematik olarak araştırılması hala eksiktir.

Bu çalışmada, akışkanlaşma deneyleri 5 farklı çaptaki kolonlar ile farklı yoğunluk ve boyuttaki 23 farklı küresel malzeme ile gerçekleştirilmiştir. Deneylerden önce malzeme karakterizasyonu yapılmıştır. Sıvı olarak musluk suyu kullanılmıştır. Bu çalışmadaki önemli bir nokta, su sıcaklığının ısıtmalı/soğutmalı su banyosu ile 20 °C’de tutulmaya çalışılmış olmasıdır. Deneylerden elde edilen veriler literatürdeki denklemler ile değerlendirilmiştir. Bu denklemler şunlardır: Akgiray ve Soyer (2006), Richardson ve Zaki (1954), Khan ve Richardson (1990), Garside ve Al-Dibouni (1977) and Hashizume ve Matsue (1998).

5 farklı kolon ve 23 farklı malzeme ile 115 farklı akışkanlaşma deneyi mümkün olmuştur. Sadece 1 cm kolondaki 10 mm cam küreler, kürelerin kolonda sıkışıp hareketsiz kalabileceği sebebiyle denenememiştir. Homojen akışkanlaşma 0,33 d/D oranından daha yüksek değerlerde mümkün olmamıştır. 0,25 ve 0,33 aralığındaki d/D oranlarında ise kolona dışarıdan kuvvetli bir vurma ile sağlanabilmiştir. Kolon çapının yatak genişlemesi üzerindeki etkisi her zaman homojen akışkanlaşmanın gerçekleştirilebildiği en küçük kolonda belirgin olarak görülmektedir. 0,2 den büyük d/D oranı için yatak genişlemesi üzerindeki duvar etkisi belirgin olarak görünürken, 0,11 ve 0,2 arasındaki d/D oranlarında daha az duvar etkisi vardır. 0,11’den küçük d/D oranları için ise duvar etkisi önemsizdir. 4000’in üzerinde deney noktası kaydedilerek yürütülen bu çalışmanın sıvı-katı akışkanlaşmasında duvar etkileri üzerine odaklanan en sistematik ve en kapsamlı tek çalışma olduğu düşünülmektedir.

Haziran, 2017

Özlem Kaplan

SYMBOLS

A : Column area

Ar : Archimedes number

α : An equation exponent as a function of $Re_{t\infty}$

D : Column diameter

d : Particle diameter

d_{eq} : Equivalent volume diameter

d_p : Particle diameter

ε : Porosity

ε_0 : Porosity of fixed bed

g : Gravitational acceleration

Ga : Galileo number

L : Depth of the expanded bed

L_0 : Depth of the fixed bed

m : Weight of particle

mx : Total weight

mp : weight of a single bead

M_p : Mass of particles

μ : Dynamic viscosity of fluid

n : Richardson-Zaki coefficient

Q : Flow rate through the filter bed

Re : Reynolds number

Re_1 : Modified Reynolds number

Re_p : Particle Reynolds number

Re_t : Reynolds number based on terminal settling velocity

$Re_{t\infty}$: Reynolds number based on terminal settling velocity in an infinite column

ρ : Density of fluid

ρ_p : Particle density

T : Temperature

V : Velocity

V_0 : Velocity free of wall effect

V_i : Intercept velocity

V_p : Volume of the particle

$V_{t\infty}$: Settling velocity of the particle in an infinite column

φ : Dimensionless value as a function of Re_1

ψ : Sphericity coefficient

ABBREVIATIONS

CA : Cellulose Acetate

GB : Glass Ball

hp : Horse Power

ID : Internal Diameter

PVC : Polyvinyl chloride



LIST OF FIGURES

Figure 1.1 Comparison of two different correlation.....	11
Figure 2.1 Actual internal diameter determinations of columns with digital caliper	13
Figure 2.2 Fluidization columns	14
Figure 2.3 Calming section.....	15
Figure 2.4 Calming section trials.....	15
Figure 2.5 Experimental Setup	17
Figure 2.6 Initial bed height trials	18
Figure 2.7 An image of glass spheres.....	20
Figure 2.8 An image of cellulose acetate spheres.....	20
Figure 2.9 An image of plastic, delrin and PVC spheres.....	21
Figure 2.10 Use of the digital micrometer.....	24
Figure 2.11 Density measurement using water displacement method	24
Figure 3.1. Three examples of homogeneous fluidization	29
Figure 3.2 Bed fragmentation and formation of cracks in 1 cm column with 5 mm CA balls.....	31
Figure 3.3 Bed fragmentation and formation of cracks.....	32
Figure 3.4 Experimental porosity values for 2 mm glass balls in 5 columns.....	33
Figure 3.5 Experimental porosity values for 7 mm glass balls in 3 columns.....	34
Figure 3.6 Porosity graph of 6 mm CA	36
Figure 3.7 Porosity graph of 2.5 mm Plastic	37
Figure 3.8 Porosity graph of 2.8 mm Plastic	38

LIST OF TABLES

Table 1.1 Velocity-voidage relations for spheres (Akgiray & Soyer, 2006).....	5
Table 2.1 Diameter of materials	19
Table 2.2 Equivalent diameter measurement.....	22
Table 2.3 Micrometer measurement results for 8 mm GB	23
Table 2.4 Example of a density measurement results.....	25
Table 3.1 Density determination results	26
Table 3.2 Equivalent diameter measurement results	27
Table 3.3 Micrometer measurement results.....	28
Table 3.4 Properties of the media used and occurrence of non-homogeneities (Note: Re _{t∞} values listed here are for ~20 °C.)	30

1 INTRODUCTION

There is a number of applications of liquid-solid fluidization in engineering (Epstein, 2003b). The most important application in Environmental Engineering is expansion of filter media during backwashing process (Soyer & Akgiray, 2009). The fluidized-bed reactors used in wastewater treatment are another type of application with an increasing interest. In order to design such systems appropriately, fluidization principles must be understood and bed expansion as a function of liquid velocity must be predicted. An aspect of liquid-solid fluidization that has not been investigated in a satisfactory manner so far is the existence and the extent of wall-effects.

Countless equations have been suggested for the prediction of the expansion of liquid fluidized beds with spherical materials. These equations were reviewed and listed in Leva (1959), Couderc, (1985), Hartman et al. (1989), Di Felice (1995), Epstein (2003), and Akgiray & Soyer (2006). An examination of the models (Richardson & Zaki, 1954; Neuzil, & Hrdina 1965; Dharmarajah & Cleasby, 1986; Garside & Al-Dibouni, 1977; Hashizume & Matsue, 1998, Khan & Richardson, 1990) that include the ratio d/D as a variable shows that there is no agreement with regard to the presence, significance, or magnitude of wall effects in liquid-solid fluidization. Di Felice (1995), for example, states that “it is doubtful if the factor d/D has any significant influence at all.” As a matter of fact, many investigators proposed expansion models that ignore wall-effects completely (Di Felice, 1995; Epstein, 2003).

An examination of the models in the literature shows that there is no agreement with regard to the presence, significance, or magnitude of wall effects in liquid-solid fluidization.

Development of a model for the prediction of wall-effects so that lab-scale data can be used to predict the behavior of full-scale equipment was the main goal of this research. In this study, a comprehensive experimental investigation of wall effects was carried out. Fluidization experiments were carried out using five columns with different diameters and a large number of solid media with varying sizes and densities. Particle characterization was performed for all particles. Tap water was used as fluid due to the ease of use and availability of tap water. Results of this investigation are valid not only

for water but also other liquids because all data gathered from the experiments were expressed in terms of dimensionless parameters like the Reynolds number. While backwash hydraulics of rapid filters used in the treatment of drinking water and wastewater is very important for this work, conclusions of this work is valid and applicable in the field of liquid-solid fluidization. This work is also expected to lead to the development of a reliable and accurate prediction method for the expansion of rapid filter media during backwashing.

1.1 Characterization of Filter Media

The particle characteristics such as size, density, shape, and surface morphology must be found before the experiments. There are many different procedures to characterize the particles. But some methods are more suitable than others for certain selected applications. So the most appropriate method should be selected for the characterization.

1.1.1 Particle density

Particle density must be known when the data obtained from the experiments are about to evaluate. Particle density affects the filtration performance and backwash flow requirements for a filter medium. High density particles need higher wash rates. And pump selection can be decided according to this. Equation 1.1 is an established formula to find the density of the material.

$$\rho_p = \frac{M_p}{V_p} \quad (1.1)$$

ρ_p =particle density

M_p =particle weight

V_p =particle volume by water displacement

1.1.2 Particle size

The particle size is one or more linear dimensions defined to characterize a single particle. As an example a sphere is characterized by its diameter. Regular shaped particles other than sphere may be characterized by two or three dimensions.

The most reliable method for diameter of a spherical material is the volume equivalent diameter (d_{eq}). Volume equivalent diameter is the diameter of a sphere having the same volume as the particle. Equation 1.2 is used to find the volume d_{eq} using V_p that is the particle volume.

$$d_{eq} = \sqrt[3]{\frac{6 \cdot V_p}{\pi}} \quad (1.2)$$

1.1.3 Particle shape

The sphericity is 1 for a sphere whereas it is always less than 1 for nonspherical particles. The sphericity was taken as 1 in the evaluation of data since all the materials in this study were spherical particles.

1.2 Fluidization of spherical particles

The selection of water velocity for the backwashing of filter bed is an important design criterion in filtration systems. Main purpose in backwash process is cleaning the filter bed so chosen velocity must be enough to fluidize the filter bed. Namely, desired expansion must be ensured with the chosen velocity for cleaning. But, high backwash velocities may cause of escaping the filter material which is an undesirable situation for the operation of filter beds. In addition, high backwash velocity means that waste of energy. There are some parameters like particle shape, particle density, water temperature and viscosity that impacts on backwash velocity. Some correlations in the literature are used to determine the optimum backwash velocity according to bed expansion of filter.

The average porosity formula is showed in Equation 1.3.

$$\frac{L}{L_0} = \frac{(1-\epsilon_0)}{(1-\epsilon)} \quad (1.3)$$

ε =Expanded bed average porosity

ε_0 =Fixed bed porosity

L =Expanded bed depth

L_0 =Fixed bed depth

Using the average porosity value, bed expansion based on velocity is predicted with the Richardson & Zaki (1954) equation:

$$\frac{V}{V_i} = \varepsilon^n \quad (1.4)$$

V =Liquid velocity, V_i =Intercept velocity

The dimensionless groups which are Reynolds number (Re) and Galileo number (Ga) are defined in equations 1.5, and 1.8.

$$Re = \frac{V \cdot \rho \cdot d}{\mu} \quad (1.5)$$

ρ =Liquid density, d =Particle diameter, μ =Liquid viscosity

$$Re_t = \frac{V_t \cdot \rho \cdot d}{\mu} \quad (1.6)$$

Re_t =Reynolds number based on terminal falling velocity

$$Re_{t\infty} = \frac{V_{t\infty} \cdot \rho \cdot d}{\mu} \quad (1.7)$$

$Re_{t\infty}$ =Reynolds number based on terminal falling velocity in an infinitely large container

$$Ga = \frac{d^3 \cdot \rho \cdot (\rho_p - \rho) \cdot g}{\mu^2} \quad (1.8)$$

Ga =Galileo number, ρ_p =Particle density

Following table (Table 1.1) which is given in Akgiray & Soyer (2006) is widely used for velocity-voidage relations for particulate, liquid fluidized beds of spheres.

Table 1.1 Velocity-voidage relations for spheres (Akgiray & Soyer, 2006)

Authors	Correlation
Richardson & Zaki (1954)	$\frac{V}{V_t} = \varepsilon^n$ where $n = 4.65 + 20 * \frac{d}{D}$ ($Re_{t\infty} < 0.2$)
Richardson (1971)	$n = 4.65 + 20 * \frac{d}{D}$ ($Re_{t\infty} < 0.2$)
	$n = \left(4.4 + 18 * \frac{d}{D}\right) Re_{t\infty}^{-0.03}$ ($0.2 < Re_{t\infty} < 1$)
	$n = \left(4.4 + 18 * \frac{d}{D}\right) Re_{t\infty}^{-0.1}$ ($1 < Re_{t\infty} < 200$)
	$n = 4.4 * Re_{t\infty}^{-0.1}$ ($200 < Re_{t\infty} < 500$)
	$n = 2.4$ ($Re_{t\infty} > 500$)
Wen & Yu (1966)	$\varepsilon^{4.7} * Ga = (18 * Re + 2.7 * Re^{1.687})$
Riba & Couderc (1977)	$d * Ga / Re^c = (a * f(\varepsilon))^c$ where $a = 1.21, b = 1.28$ if $\varepsilon < 0.85$, $a = 0.77, b = 2.70$ if $\varepsilon > 0.85$; $c = 1, d = 1/18, e = 1$ if $Ga < 18$ $c = 1.4, d = 1/13.9, e = 1.4$ if $18 < Ga < 10^5$; $c = 2, d = 3, e = 2$ if $Ga > 10^5$ $f(\varepsilon) = (1 - 1.21 * (1 - \varepsilon)^{2/3})^{-1}$
Garside & Al-Dibouni (1977)	$\varepsilon^{5.14} + 0.048 * \varepsilon^{2.28} * Re_t^{\varepsilon+0.2} = \frac{Re * (1 + 0.06 * Re_t^{\varepsilon+0.2})}{Re_t}$ if $\varepsilon \leq 0.85$
	$\varepsilon^{5.14} + 0.06 * \varepsilon^{3.65} * Re_t^{\varepsilon+0.2} = \frac{Re * (1 + 0.06 * Re_t^{\varepsilon+0.2})}{Re_t}$ if $\varepsilon > 0.85$
Gibilaro et al., (1986)	$\varepsilon^{4.8} * Ga = Re^2 * ((17.3/Re)^\alpha + 0.336^\alpha)^{1/\alpha}$ $\alpha = 2.55 - 2.1 * \left[\tanh * (20 * \varepsilon - 8)\right]^{1/3}$
Khan & Richardson (1990)	$\frac{V}{V_t} = \varepsilon^n$ $V/V_{t\infty} = 1 - 1.15 * (d/D)^{0.6}$ $\frac{4.8-n}{n-2.4} = 0.043 * Ga^{0.57} \left[1 - 1.24 * \left(\frac{d}{D}\right)^{1.27}\right]$

Akgiray & Soyer (2006), developed an equation with a simple form for the prediction of bed expansion in liquid fluidized beds of spheres.

$$\phi = k_1 * Re_1 + k_2 * Re_1^P \quad (k_1=3.137, k_2=0.673, P=1.766)$$

$$\log \phi = \log(k_1 * Re_1 + k_2 * Re_1^P)$$

$$\log \phi = \log(3.137 * Re_1 + 0.673 * Re_1^{1.766}) \quad (1.9)$$

ϕ =Dimensionless value as a function of Re_1

Re_1 =Modified Reynolds number

$$\phi = \frac{\epsilon^3}{(1-\epsilon)^2} * \frac{\Psi^3 * d_{eq}^3 * \rho * (\rho_p - \rho) * g}{216 * \mu^2} \quad (\text{Richardson \& Meikle, 1961}) \quad (1.11)$$

Ψ =Sphericity

g = Gravitational acceleration (9.81 m/sec²)

$$Re_1 = \frac{\Psi * d_{eq} * \rho * V}{6 * \mu * (1-\epsilon)} \quad (1.12)$$

Hashizume & Matsue (1998) report a method to predict the void fractions concerning the wall effect of column. Their method is based on experimental results and they use some existing correlations for their method. This method is explained below.

Re_t is obtained by using equations below.

$$\log Re_{t\infty} = P + \log R \quad (1.13)$$

$$P = [(0.0017795 * A - 0.0573) * A + 1.0315] * A - 1.26222 \quad (1.14)$$

$$R = 0.99947 + 0.01853 * \sin(1.848 * A - 3.14) \quad (1.15)$$

$$A = \log Ar \quad (\text{Hartman et al., 1989}) \quad (1.16)$$

Ar =Archimedes number

Re_t is corrected by using equation 1.17.

$$\frac{Re_t}{Re_{t\infty}} = 1 - 0.75 * \left(\frac{d}{D}\right)^{0.4} \quad (1.17)$$

Equation 1.18 gives the n with the equation 1.19.

$$\frac{n}{n_{\infty}} = 1 - 0.75 * \left(\frac{d}{D}\right) \quad (1.18)$$

$$\frac{(4.8 - n_{\infty})}{(n_{\infty} - 2.4)} = 0.043 * Ar^{0.57} : d/D \leq 0.01 \quad (1.19)$$

The void fraction is obtained from equation 1.20 using the Re_t and n .

$$\frac{Re_p}{Re_t} = \varepsilon^n \quad (1.20)$$

Re_p = Particle Reynolds number

ε_{mf} should be known because the void fraction cannot be smaller than at ε_{mf} and calculated as follows.

$$\varepsilon_{mf} = 1 - \frac{V_p}{(A_D * H_{mf})} \quad (1.21)$$

ε_{mf} = Void fraction at minimum fluidization

H_{mf} = Bed height of minimum fluidization

V_p = Particles volume

A_D = Cross-sectional area of the column

Finally, Hashizume & Matsue (1998) express their data with equation 1.22.

$$\varepsilon_{mf} = 0.46 + 0.03 \log\left(\frac{d}{D}\right) \quad (1.22)$$

1.3 Wall effects in liquid-solid fluidization

Container wall effects may be significant in fluidization when the ratio (d/D) of the particle size to container diameter is large. According to a number of literature sources (e.g. Wilhelm & Kwauk, 1948; Loeffler, 1953), a given porosity is attained in a small-diameter column at a fluidization velocity lower than the velocity required in an “infinitely large” container provided that all other conditions are the same. Put in other words, for a given fluidization velocity, the porosity observed in a small-diameter column will be higher than that observed in a column with a larger diameter. While the wall effect of container is probably insignificant in most industrial operations, it may be

important in laboratory experiments. Wall effects, therefore, should be given careful consideration when (1) data provided from small columns are used to derive a formula intended for application to large full-scale equipment, or (2) a formula directly practicable only to large columns is to be employed to small columns. The following situations are examples of the second case: (i) understanding and interpretation of data obtained from lab-scale columns, (ii) the use of a large number of small columns in parallel in a full-scale operation. Some fluidization systems used for heat transfer is an example of the latter situation (Hashizume & Matsue, 1998).

The term “wall effect” is used with more than one connotation in systems where granular materials and fluids are in contact. The following classification may be made based on the properties and events influenced by the presence of walls in such systems:

1. Settling velocity of a single discrete particle in a fluid
2. Porosity of fixed beds of particles
3. Head loss (pressure loss) in fixed beds due to flow
4. Porosity and bed expansion in fluidized beds.

In addition to these, there can be “wall effects” on the efficiency of lab-scale or pilot-scale systems involving filtration, ion exchange or adsorption. Existing models for wall-effects in fixed-bed head loss calculations are explained and compared in a recent study (Erdim et al., 2015).

As to when wall effects become significant in fluidization, two approaches have been taken in the literature. Some investigators indicated that a critical value of d/D exists. Many different values such as $1/15$, $1/20$, $1/50$, $1/100$, $1/200$ were suggested by a number of investigators (Neuzil & Hrdina, 1965, Khan & Richardson, 1990; Epstein, 2003). According to the Richardson-Zaki correlation (Richardson & Zaki, 1954; Richardson & Meikle, 1961; Richardson et al., 1971), however, wall effects depend on both $Re_{t\infty}$ and d/D . ($Re_{t\infty} = V_{t\infty}\rho d/\mu$ is the Reynolds number found from the terminal settling velocity $V_{t\infty}$ of an isolated particle in an column at infinite width, and should not be confused with the Reynolds number Re found from the superficial fluidization velocity.) Dharmarajah & Cleasby (1986) analyzed the data by Loeffler (1953) and also determined that effect of container wall depends on both $Re_{t\infty}$ and d/D . They have

showed the subsequent curve-fitting formula based on the actual backwash velocity V and a hypothetical backwash velocity V_0 which is free of wall effects:

$$\frac{V_0}{V} = 10^{\alpha*(d/D)} \quad (1.2)$$

$$\text{where } \alpha = 5.18 / \text{Re}_{t\infty}^{0.585} \quad (1.24)$$

V_0 is the backwash velocity required to achieve the same porosity in a column at infinite width while velocity V would produce in a column of diameter D .

An examination of the models in the literature shows that there is no agreement with regard to the presence, significance, or magnitude of wall effects in liquid-solid fluidization. To exemplify the disagreement between different investigators, it will be useful here to compare the wall-effect predicted by the Richardson-Zaki correlation with that predicted by the Dharmarajah-Cleasby approach. For fluidization, the Richardson-Zaki formula can be written as follows:

$$\frac{V}{V_t} = 10^{-d/D * \epsilon^n} \quad (1.25)$$

where V and ϵ are the fluidization velocity and expanded porosity, respectively, in the column with a diameter D , whereas V_t indicates the terminal settling velocity of an one spherical bead in a column at infinite width. The n index in this equation is calculated with following equations (Richardson et al., 1971):

$$n = (4.4 + 18 * \frac{d}{D}) \text{Re}_t^{-0.03} \quad \text{for } 0.2 < \text{Re}_t < 1 \quad (1.26)$$

$$n = (4.4 + 18 * \frac{d}{D}) \text{Re}_t^{-0.1} \quad \text{for } 1 < \text{Re}_t < 200 \quad (1.27)$$

$$n = 4.4 * \text{Re}_t^{-0.1} \quad \text{for } 200 < \text{Re}_t < 500 \quad (1.28)$$

$$n = 2.4 \quad \text{for } 500 < \text{Re}_t \quad (1.29)$$

The limit $d/D \rightarrow 0$ is taken in order to estimate the velocity (V_0) that would give the value ϵ in an infinitely large column. Therefore, according to this model,

$$\frac{V_0}{V_t} = \epsilon^{n_0} \quad (1.30)$$

and

$$\frac{V_0}{V} = 10^{d/D} * \epsilon^{n_0-n} \quad (1.31)$$

where n_0 is obtained by setting $d/D = 0$ in the Richardson-Zaki model:

$$n_0 - n = -20 * \frac{d}{D} \quad \text{for } Re_t < 0.2 \quad (1.32)$$

$$n_0 - n = -18 * \frac{d}{D} * Re_t^{-0.03} \quad \text{for } 0.2 < Re_t < 1 \quad (1.33)$$

$$n_0 - n = -18 * \frac{d}{D} * Re_t^{-0.1} \quad \text{for } 1 < Re_t < 200 \quad (1.34)$$

$$n_0 - n = 0 \quad \text{for } 200 < Re_t \quad (1.35)$$

Comparing this model with the Dharmarajah-Cleasby equation, the following can be concluded. (i) According to the Dharmarajah-Cleasby approach, the wall effect is independent of porosity, whereas the Richardson-Zaki model predicts that V_0/V depends on porosity unless $200 < Re_t$. (ii) The Dharmarajah-Cleasby approach predicts that a wall effect is absent for large Re_t , i.e. $V_0/V \rightarrow 1$ as $Re_t \rightarrow \infty$. On the other hand, according to the Richardson-Zaki model, $V_0/V \rightarrow 10^{d/D}$ as $Re_t \rightarrow \infty$. (iii) The Dharmarajah-Cleasby approach predicts dependence on both Re_t and d/D for all values of Re_t , whereas in the Richardson-Zaki model V_0/V depends only on d/D for $Re_t < 0.2$ and for $200 < Re_t$. (iv) Another important difference between the two approaches is that, the Richardson-Zaki equation predicts that V_0/V remains constant and independent of Re_t for $Re_t < 0.2$. This contradicts the Dharmarajah-Cleasby equation which predicts increasing V_0/V values as Re_t decreases. As a matter of fact, the application of the Dharmarajah-Cleasby wall-effect correction method for small values of Re_t may lead to very large errors. (v) The V_0/V curves calculated using the Richardson-Zaki equation contain two jump discontinuities (at $Re_t=0.2$ and $Re_t=200$). From a physical point of view, this feature of the Richardson-Zaki model is not reasonable.

From what has been said above, it is clear that the two approaches not only disagree quantitatively, but they are qualitatively inconsistent and both equations cannot be generally valid. This can be better appreciated by inspecting the following figure (Figure 1.1). This figure shows how the ratio V_0/V changes with Re_t . These curves have been calculated for $d/D = 0.01$. It may be noted that the Richardson-Zaki equation leads

to a different curve for each different value of porosity.

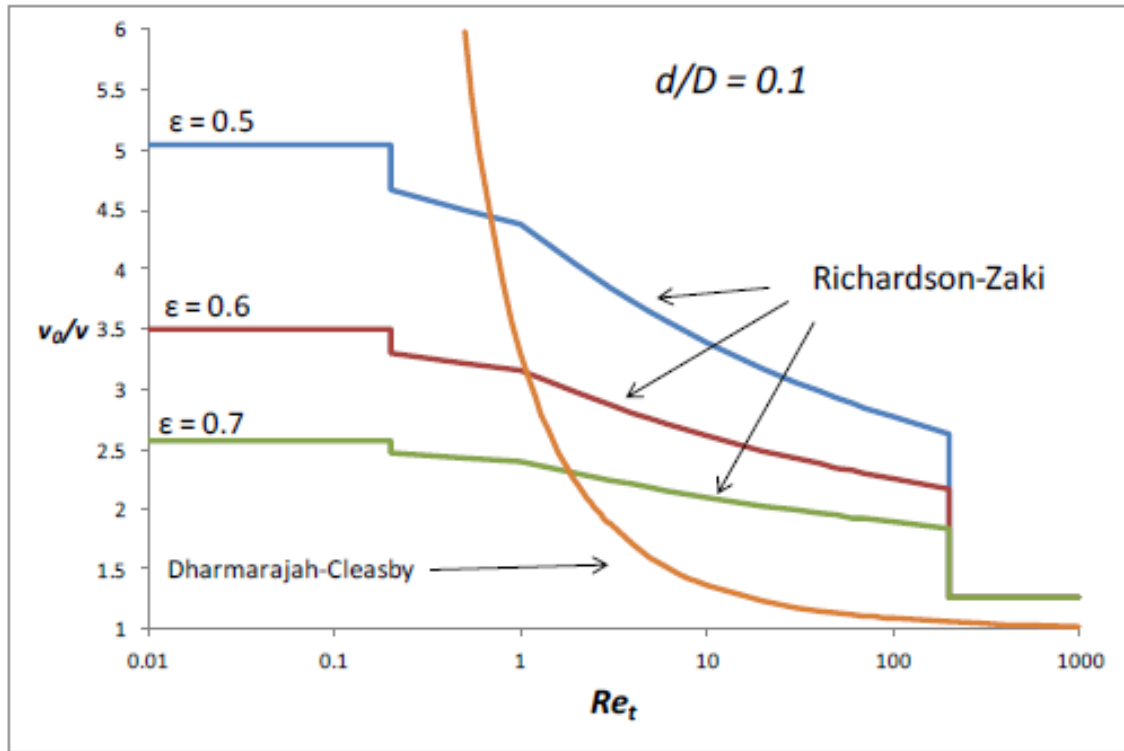


Figure 1.1 Comparison of two different correlation

Di Felice (1995) stated that the kind of strong wall effect predicted by the Richardson-Zaki correlation “has not been confirmed subsequently and it is doubtful if the factor d/D has any significant influence at all.” Furthermore, the wall-effect correction terms in a modified form of the Richardson-Zaki correlation published by Khan & Richardson (1990) are significantly different from those of the original Richardson-Zaki equations. Notable among the other fluidization models that attempt to account for wall effects are those proposed by Rowe (1987) and Garside & Al-Dibouni (1977). It can be shown that the Richardson-Zaki model, the more recent Khan-Richardson model, and the model proposed by Garside and Al-Dibouni do not fit Loeffler's (1953) wall-effect data well. (Furthermore, the latter two models lead to an anomaly that may not have been noticed by their authors: V_0/V versus Re_t curves calculated according to these models go through maximum points.) Many other investigators, on the other hand, proposed models that ignore wall-effects completely (Di Felice, 1995; Epstein, 2003).

To summarize, there is no agreement in the fluidization literature regarding (i) the

presence and significance of wall-effects in liquid-solid fluidization, and (ii) how wall-effects should be taken into account. One reason for this lack of a good understanding of wall-effects is that they have not been subjected to a systematic and conclusive experimental investigation. Since the pioneering work of Wilhelm & Kwauk (1948) and Loeffler (1953), the only notable study of wall-effects in fluidization was carried out by Neuzil & Hrdina (1965) and Hashizume & Matsue (1998). Unfortunately, as noted by Dharmarajah (1982), these latter investigators did not present their results in a useful and understandable manner.



2 MATERIALS AND METHOD

Laboratory devices, equipment, and methods which were used in the fluidization experiments and particle characterization are detailed in this section.

2.1 Experimental Setup

Fluidization experiments were carried out using 23 different solid materials with varying sizes and densities in order to ascertain the effect of column size on the behavior and expansion of the different particles during fluidization. To allow the collection of data at high expansions as well as low expansions, 1.5 m deep plexiglass columns were employed. There were 5 columns whose nominal internal diameters are 1 cm, 2 cm, 3 cm, 4 cm and 5 cm. But actual internal diameters were carefully determined with calibrated digital caliper (TED PELLA, INC) and measured values were used for calculations instead of nominal values (Figure 2.1). Because internal diameter of columns affect the porosity indeed.

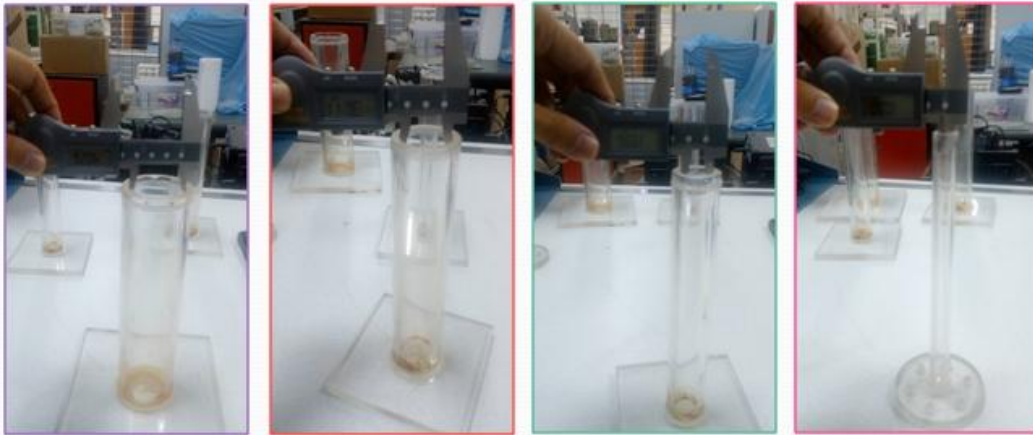


Figure 2.1 Actual internal diameter determinations of columns with digital caliper

Preparation of fluidization columns: firstly the columns were checked against any leakage and consolidated with a water resistant adhesive. Then the ruler was properly placed on the column so that the water level could be read. The columns were mounted to the wall with clamps as perpendicular. Plastic pipes were supplied with the valves at the inlet and outlet of the column. All five columns can be seen in Figure 2.2.

There were sections called as calming or homogenizing section (Yang, 2003) having the



Figure 2.2 Fluidization columns

same diameter as fluidization part at the entrance and the outlet of the column. Both of these sections are 25 cm in height and attached to the column with flanges. 100 μ screen filter was placed in these sections in order to avoid escaping of materials during the experiment. 10 mm glass beads were filled to these parts for columns have an inlet diameter of 5 and 4 cm. 3 mm glass beads were filled to these structures for columns having 3, 2 and 1 cm inlet diameter. Inlet section makes water to distribute to the column homogeneously. An example of a calming section is shown in Figure 2.3.

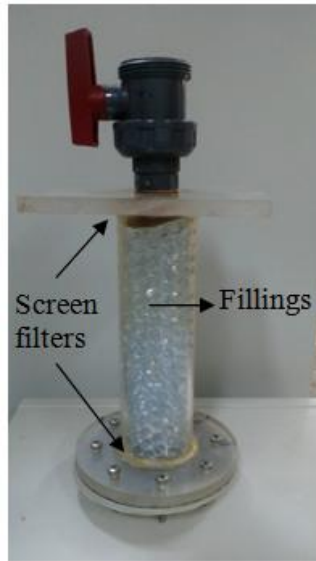


Figure 2.3 Calming section

Some experiments with fillings and without fillings were tried to examine the effect of calming section at the outlet of the column. Figure 2.4 shows that there was no effect of fillings on the results.

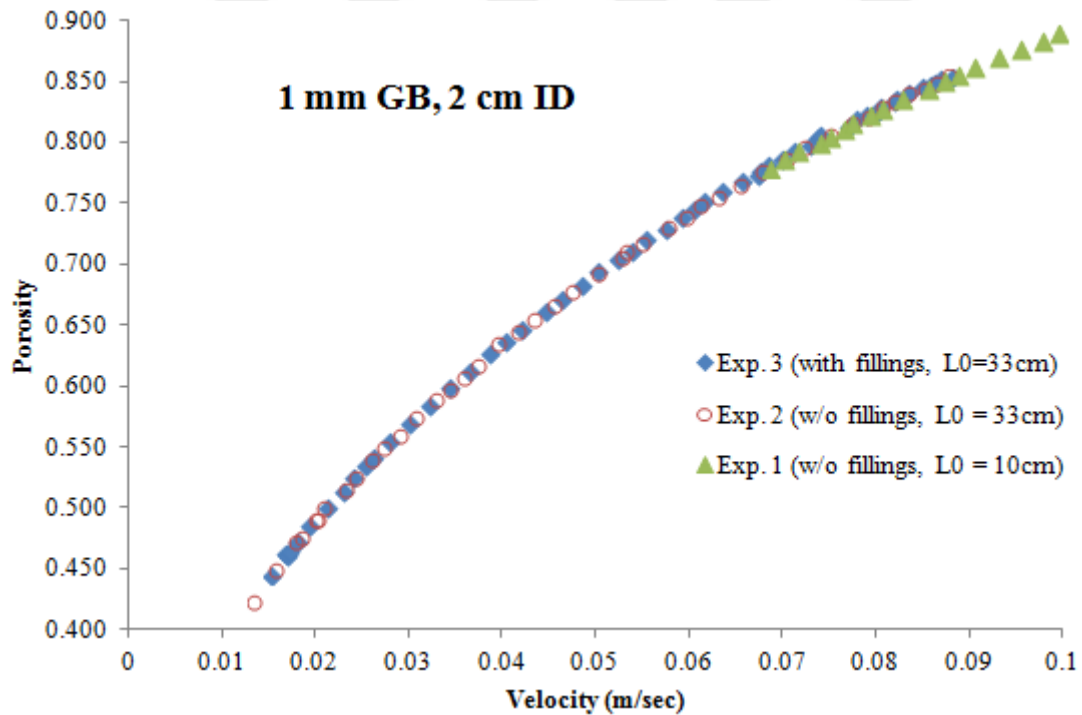


Figure 2.4 Calming section trials

At the beginning of the experiments, tap water was filtered from 5 μ and 1 μ filter, taken to a 100-liter cylindrical tank and used in experiments. It was always aimed to keep the water temperature at 20 °C by the help of recirculating chiller/heater bath (Labo B100-H23). A centrifugal pump (SUMAK-SMT300/2) which has 3 hp pump power and frequency controller was selected and operated. Bed expansion as a function of fluidization velocity was measured during each experiment. Water temperature and flow rate were monitored and recorded for each measurement in all the experiments. The amount of water taken for a certain period with a chronometer was weighed and then the flow rate was found. Water temperature was measured with a very sensitive thermometer (Anton Paar-MK50). Experimental setup is showed in Figure 2.5.

The filter material is weighed and placed to the column. About 10 cm of initial bed heights were generally same in all columns. The flow rate is increased carefully and gradually during experiments. There should not be bubbles on filter materials or anywhere in the system. The bed is first fluidized to the highest level to get rid of the bubbles in column or pipe which returns back water to the tank. In addition, filter materials except glass beads are held in water for 24 hours in order to wet the surface of the material so bubble formation is avoided. Expanded bed height is recorded from the ruler which is attached to the columns when the level is stable. The column must be vertical in flat to read the level correctly. There was no one single sharp level every time. The minimum and maximum levels were recorded for data points which fluctuations occurred in.

The most effective initial bed height were determined with some experiments carried out using different initial bed height values of 5 cm, 10 cm, 15.15 cm, 20 cm, and 28.8 cm (Figure 2.6). About 10 cm initial bed height was the most appropriate one because data regarding to highest expansion values could be collected. The reason why the initial bed height of 5 cm was not chosen is that jet flow could occur from the bottom of the column and homogeneous fluidization cannot be ensured.

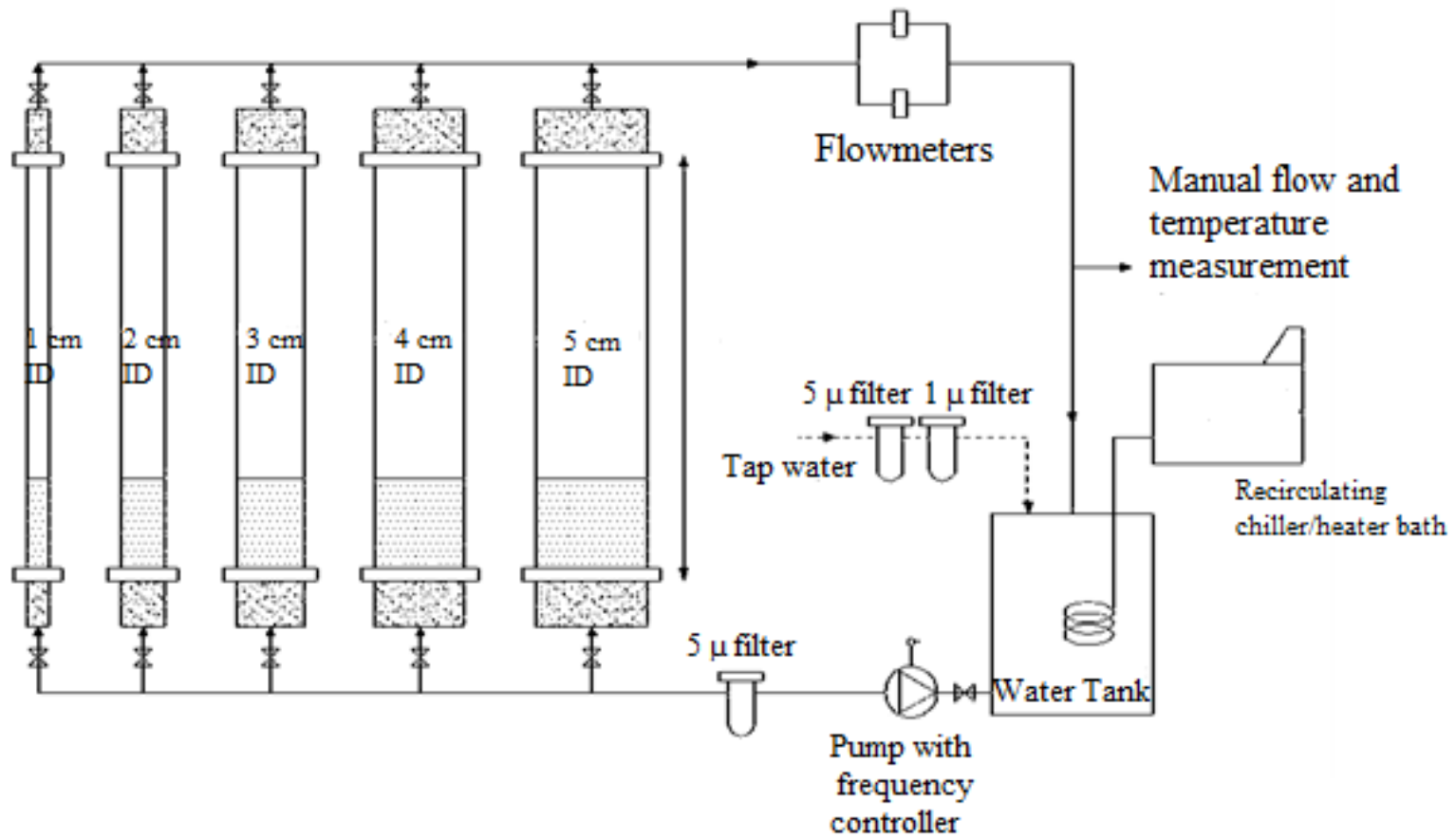


Figure 2.5 Experimental Setup

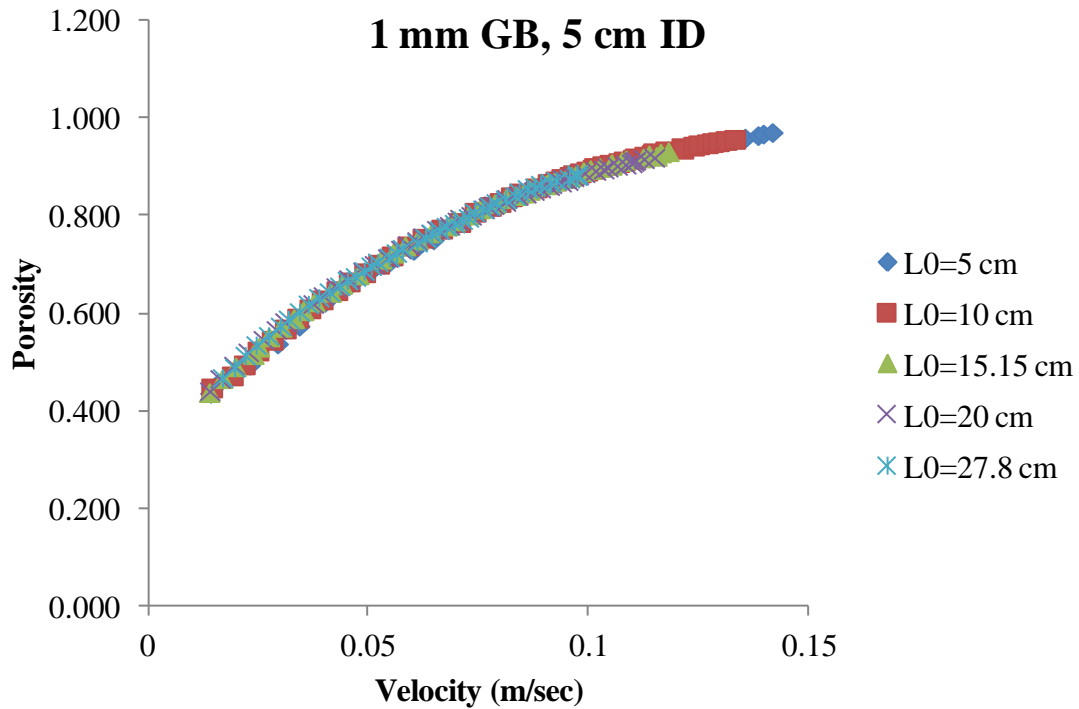


Figure 2.6 Initial bed height trials

Dynamic viscosity and density of water are found from the water temperature. The equation below is used to find the density (Weast et al., 1989).

$$\rho = (999.83952 + (16.945176 * T) - (7.9870401E-3 * T^2) - (4.6170461E-5 * T^3) + (1.0556302E-7 * T^4) - (2.8054253E-10) * T^5) / (1 + 0.01687985 * T) \quad (2.1)$$

ρ = density of water (kg/m^3), T = temperature of water ($^{\circ}\text{C}$)

The equations below are used to find the dynamic viscosity (Weast et al., 1989).

$$\mu = 10^{-3} * 10^{\left(\frac{1301}{(998.333 + 8.1855 * (T - 20) + 0.00585 * (T - 20)^2) - 1.30233} \right)} \text{ for temperature values are lower than or equal to } 20^{\circ}\text{C}, \quad (2.2)$$

$$\mu = 10^{-3} * 10^{\left(\frac{1301}{(998.333 - 1.30233)} \right)} \text{ for temperature values are greater than } 20^{\circ}\text{C}, \quad (2.3)$$

μ = dynamic viscosity of water ($\text{kg}/\text{m}/\text{sec}$)

2.2 Materials

Glass, cellulose acetate, delrin, PVC and plastic balls of varying sizes and densities were employed in the experiments. These spherical particles are listed in Table 2.1.

Table 2.1 Diameter of materials

Materials	Nominal Diameters (mm)	Actual Diameters (mm)
Glass balls	1	1.19
Glass balls	2	2.02
Glass balls	3	3.18
Glass balls	4	4.01
Glass balls	5	4.98
Glass balls	6	6.03
Glass balls	7	7.15
Glass balls	8	8.02
Glass balls	10	9.99
Cellulose Acetate (yellow)	2.5	2.43
Cellulose Acetate (black)	3	3.01
Cellulose Acetate (red)	3.5	3.48
Cellulose Acetate (brown)	4.5	4.45
Cellulose Acetate (white)	5	4.93
Cellulose Acetate (white)	6	5.97
Delrin	2.4	2.38
Delrin	3.2	3.18
Delrin	4	3.97
Delrin	4.8	4.76
Plastic (orange) balls	2	1.97
Plastic (brown) balls	2.5	2.48
Plastic (blue) balls	3	2.86
PVC	4.8	4.79

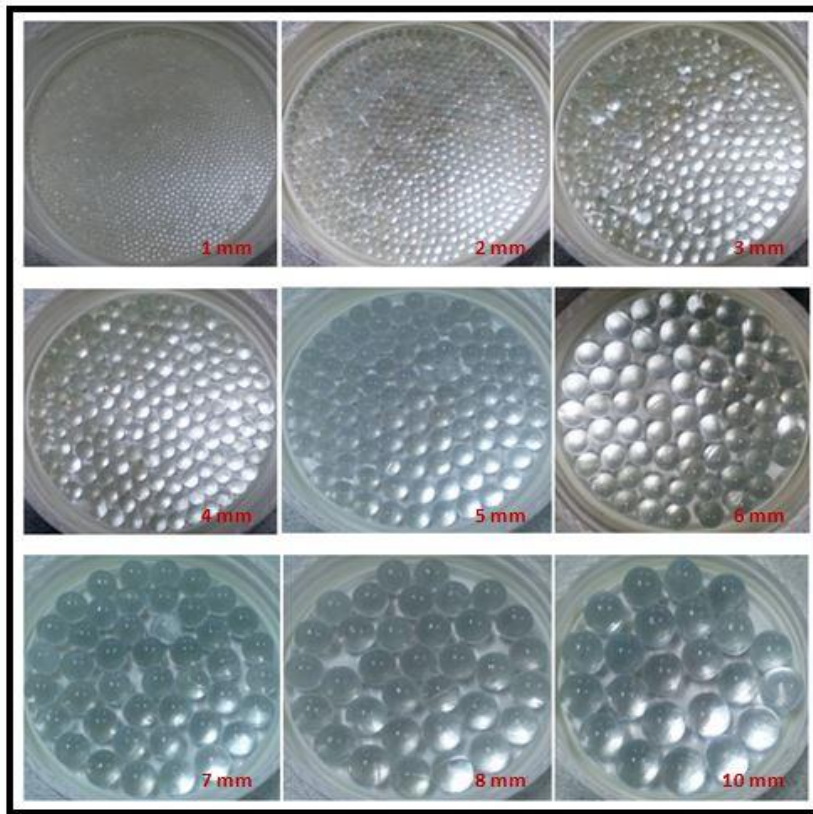


Figure 2.7 An image of glass spheres



Figure 2.8 An image of cellulose acetate spheres

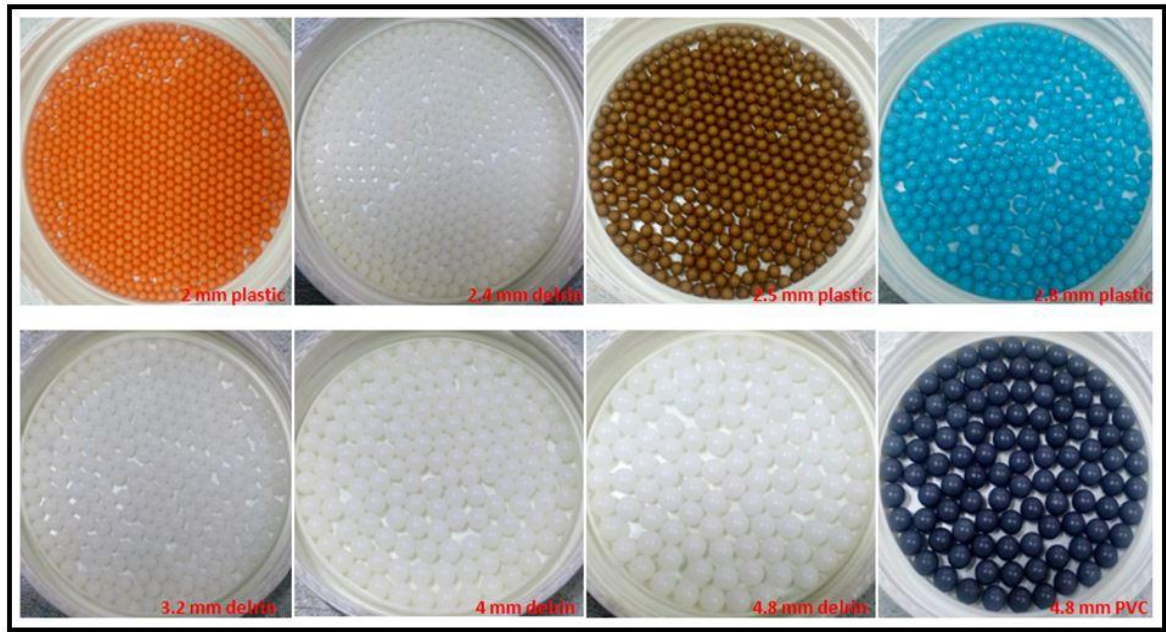


Figure 2.9 An image of plastic, delrin and PVC spheres

2.3 Characterization of Materials

The physical properties of each type of particle were determined before the experiments. These physical properties are particle size and density. Pycnometer bottles were utilized for the density determination. For the particle size, equivalent diameter measurement which is a tedious weighing and counting technique was employed for each of the 23 types of particle and so particle diameters were determined.

2.3.1 Particle size

2.3.1.1 Equivalent diameter

Equivalent diameter (d_{eq}) is the diameter of a sphere that is having the same volume with the particle being measured. The equation below is used for the calculation of equivalent diameter.

$$d_{eq} = \sqrt[3]{\frac{6 \cdot m}{\pi \cdot \rho_p}} \quad (2.4)$$

m: weight of particle (gr)

ρ_p : density of particle (gr/cm³)

The calculation steps for the equivalent diameter for each particle are listed below.

1. Particles are counted as 200 grains and weighed
2. Volume of a grain is calculated from its particle density
3. Volume of one grain is equated to the volume of equivalent sphere using Equation 2.4

These steps are repeated three times for each type of material. Table 2.2 shows the results of equivalent diameter measurements

Table 2.2 Equivalent diameter measurement

Material:		8 mm Glass	
Quantity (x)	Total weight mx (g)	Weight of a single bead mp (g)	Equivalent diameter of a particle dp (mm)
200	139.2164	0.6961	8.0210
200	139.2310	0.6962	8.0213
195	135.6368	0.6956	8.0191
	Average	0.6959	8.0205
	Standard deviation		0.00122

2.3.1.2 Measurement with digital micrometer

The diameter of particles was also checked with a calibrated digital micrometer (TED PELLA, INC). 23 different particles were evaluated for these measurements and all data were recorded. Micrometer measurement results were generally consistent with the results of equivalent diameter results. An example of the micrometer measurement results was given in Table 3.3.

2.3.2 Density determination of materials

The density of filter materials must be known in order to design solid-liquid systems like systems that backwashing of granular filters and washing of soils, adsorption and ion exchange or liquid-fluidized bed heat exchangers. Water displacement method was employed to determine the particle density using pycnometer bottles. In this method, a pycnometer bottle of known volume (50 ml and 100 ml) was used.

Table 2.3 Micrometer measurement results for 8 mm GB

#	Diameter (mm)
1	8.010
2	8.000
3	8.005
4	8.110
5	8.035
6	8.000
7	7.950
8	7.900
9	8.010
10	8.000
11	8.110
12	8.100
13	7.950
14	8.175
15	8.105
16	7.900
17	8.010
18	8.025
19	7.975
20	8.040
21	8.025
22	8.100
23	8.075
24	8.040
25	8.010
Average	8.026
Standard Deviation	0.06639



Figure 2.10 Use of the digital micrometer

First weight of dry pycnometer is recorded. Then, the pycnometer is filled with water as well as a capillary hole in the stopper is filled with water. Spare water that leaks through the capillary hole is dried with a napkin and total weight is measured. Pycnometer bottle is emptied and weighed again. The material is placed to the about 1/3 of bottle and weight is recorded. Water is added to pycnometer as well as a capillary hole in the stopper is filled with water. Spare water that leaks through the capillary hole is dried with a napkin and total weight is measured. Finally, the temperature of the water is measured. This procedure is repeated 3 times for each particle and average density value is taken.



Figure 2.11 Density measurement using water displacement method

Cellulose acetate, plastic, delrin and PVC materials are waited in water for 24 hours before the last weight measurement because these types of materials keep air bubbles on their surfaces and these air bubbles make weight measurement wrong and therefore the density measurement wrong.

Table 2.4 Example of a density measurement results

Material	2.5 mm Yellow Acetate Balls		
	Temperature of water, (°C):	18.1	18.3
(1) Weight of dry pycnometer, (g)	36.6421	36.6415	36.1411
(2) Weight of pycnometer full of water, (g)	136.1273	135.9381	135.9043
(3) Weight of pycnometer inside wet, (g)	36.9262	36.9048	36.3820
(4) Weight of pycnometer inside wet + Material, (g)	80.9731	78.2121	83.9170
(5) Weight of pycnometer inside wet + Material + Water to fill, (g)	146.1462	145.3148	146.7081
(6) Weight of material = (4) - (3), (g)	44.0469	41.3073	47.5350
(7) Weight of water to fill pycnometer = (2) - (1), (g)	99.4852	99.2966	99.7632
(8) Weight of extra water to fill pycnometer over the material = (5) - (1) - (6), (g)	65.4572	67.3660	63.0320
(9) Weight of equivalent volume of water = (7) - (8), (g)	34.0280	31.9306	36.7312
(10) The specific gravity of material at tested temperature = (6) / (9)	1.29443106	1.29365875	1.29413142
(11) Density of water at tested temperature, (g/ml)	998.577042	998.539626	998.577042
(12) Density of material = (10) * (11), (kg/m ³)	1292.58914	1291.76952	1292.28993
Average density, (kg/m ³)	1292.21619		

3 RESULTS AND DISCUSSION

3.1 Particle Characterization Results

Particle characterization was carried out before starting the fluidization experiments. First, material density was found using water displacement technique. Average value of three different measurements was used in the calculations. All results regarding to density results are shown in Table 3.1. Standard deviation values are also shown in the table.

Table 3.1 Density determination results

Material	Density (g/cm ³)			Average density	Standard deviation
	1st	2nd	3rd		
1 mm Glass	2.49	2.49	2.49	2.47	0.002
2 mm Glass	2.57	2.56	2.57	2.57	0.002
3 mm Glass	2.49	2.49	2.50	2.49	0.005
4 mm Glass	2.50	2.50	2.50	2.50	0.001
5 mm Glass	2.53	2.53	2.53	2.53	0.001
6 mm Glass	2.57	2.56	2.56	2.56	0.005
7 mm Glass	2.52	2.52	2.52	2.52	0.001
8 mm Glass	2.58	2.58	2.58	2.58	0.001
10 mm Glass	2.57	2.57	2.57	2.57	0.001
2.5 mm Cellulose Acetate	1.29	1.29	1.30	1.29	0.003
3 mm Cellulose Acetate	1.28	1.29	1.28	1.28	0.004
3.5 mm Cellulose Acetate	1.28	1.29	1.29	1.29	0.003
4.5 mm Cellulose Acetate	1.25	1.25	1.25	1.25	0.002
5 mm Cellulose Acetate	1.28	1.29	1.29	1.29	0.002
6 mm Cellulose Acetate	1.27	1.27	1.26	1.27	0.004
2.4 mm Delrin	1.39	1.39	1.39	1.39	0.002
3.2 mm Delrin	1.42	1.42	1.41	1.42	0.002
4 mm Delrin	1.38	1.38	1.38	1.38	0.002
4.8 mm Delrin	1.38	1.39	1.38	1.38	0.006
2 mm Plastic	1.17	1.19	1.19	1.18	0.011
2.5 mm Plastic	1.21	1.20	1.20	1.21	0.002
2.8 mm Plastic	1.19	1.19	1.19	1.19	0.002
4.8 mm PVC	1.36	1.36	1.35	1.36	0.006

Equivalent diameter measurement which is a counting and weighing technique was employed for particle diameter. Table 3.2 shows the results according to three different trials. Standard deviation values which prove the reliability of the values are also shown

in this table.

Table 3.2 Equivalent diameter measurement results

Material	Equivalent diameter (mm)			Average Equivalent diameter	Standard deviation
	1st	2nd	3rd		
1 mm Glass	1.19	1.18	1.20	1.19	0.007
2 mm Glass	2.02	2.02	2.02	2.02	0.002
3 mm Glass	3.19	3.15	3.20	3.18	0.025
4 mm Glass	4.01	4.01	4.02	4.01	0.010
5 mm Glass	4.98	4.97	4.97	4.98	0.001
6 mm Glass	6.03	6.02	6.02	6.03	0.002
7 mm Glass	7.15	7.15	7.15	7.15	0.001
8 mm Glass	8.02	8.02	8.02	8.02	0.001
10 mm Glass	9.99	9.99	9.99	9.99	0.001
2.5 mm Cellulose Acetate	2.44	2.43	2.43	2.43	0.002
3 mm Cellulose Acetate	3.01	3.01	3.01	3.01	0.001
3.5 mm Cellulose Acetate	3.48	3.48	3.48	3.48	0.000
4.5 mm Cellulose Acetate	4.45	4.44	4.45	4.45	0.002
5 mm Cellulose Acetate	4.93	4.93	4.93	4.93	0.001
6 mm Cellulose Acetate	5.97	5.97	5.97	5.97	0.001
2.4 mm Delrin	2.39	2.39	2.38	2.39	0.001
3.2 mm Delrin	3.17	3.18	3.18	3.18	0.001
4 mm Delrin	3.96	3.96	3.97	3.97	0.004
4.8 mm Delrin	4.76	4.76	4.76	4.76	0.000
2 mm Plastic	1.96	1.97	1.97	1.97	0.003
2.5 mm Plastic	2.48	2.48	2.48	2.48	0.001
2.8 mm Plastic	2.86	2.86	2.86	2.86	0.002
4.8 mm PVC	4.79	4.79	4.79	4.79	0.000

Particle diameters were also checked with a digital micrometer and results are in the Table 3.3. These results are very close to diameter values in the equivalent diameter measurement results.

Fluidization experiments were carried out with water after particle characterization. Results of the experiments were evaluated using different correlations in the literature.

Table 3.3 Micrometer measurement results

Micrometer Measurement		
Material	Diameter (mm)	Standard deviation
1 mm Glass	1.20	0.071
2 mm Glass	2.03	0.048
3 mm Glass	3.20	0.180
4 mm Glass	3.90	0.124
5 mm Glass	4.96	0.067
6 mm Glass	6.02	0.122
7 mm Glass	7.05	0.053
8 mm Glass	8.03	0.066
10 mm Glass	10.01	0.064
2.5 mm Cellulose Acetate	2.44	0.014
3 mm Cellulose Acetate	3.03	0.012
3.5 mm Cellulose Acetate	3.49	0.013
4.5 mm Cellulose Acetate	4.47	0.013
5 mm Cellulose Acetate	4.96	0.018
6 mm Cellulose Acetate	6.00	0.005
2.4 mm Delrin	2.40	0.008
3.2 mm Delrin	3.19	0.009
4 mm Delrin	3.98	0.007
4.8 mm Delrin	4.78	0.008
2 mm Plastic	1.95	0.049
2.5 mm Plastic	2.45	0.035
2.8 mm Plastic	2.79	0.094
4.8 mm PVC	4.81	0.009

3.2 Results of Fluidization Experiments

One of the most important observations in this work was that “homogeneous” fluidization could not be achieved at all in some of the experiments. This happened mostly in the 1 cm column, and in three cases in the 2 cm column (Table 3.4). All the particles were fluidized homogeneously in the 3 cm, 4 cm, and 5 cm columns. Table 3.4 therefore gives information about bed behavior (i.e. homogeneous versus non-homogeneous) only for the experiments carried out in the 1 cm, 2 cm, and 3 cm columns (the 3 cm column is also included in the table for reasons that will be clear in what follows).

The term “homogeneous” is used here somewhat loosely to refer to fluidized beds without large gaps and cracks (large void spaces) within the bed and does not necessarily imply the presence of a completely uniform porosity over the entire fluidized bed. As a matter of fact, parvoids (voidage waves travelling upwards) were visible to the naked eye in the majority of the experiments. In certain cases, e.g. with large glass balls, one could argue that first “slugging fluidization” (at lower rates) and then “turbulent fluidization” (at the highest rates) took place in the column. As long as a reproducible mean bed depth was measurable and there were no visible permanent cracks or interlocked clusters in the bed, the experiment is termed “homogeneous” here. Examples of homogeneously fluidized beds are shown in Figure 3.1. Figure 3.2 and Figure 3.3 display typical examples of non-homogeneously fluidized beds. The following types of non-homogeneity were observed in at least 16 of the 114 fluidization experiments. In Figure 3.1, first picture belongs to 5 cm column with 2.5 mm delrin balls, second picture belongs to 4 cm column with 2.5 mm CA balls, and third picture belongs to 4 cm column with 3 mm CA balls.



Figure 3.1. Three examples of homogeneous fluidization

Table 3.4 Properties of the media used and occurrence of non-homogeneities (Note: Re_{∞} values listed here are for ~ 20 °C.)

Particle no	Particle type	ρ_p (gr/cm ³)	d (mm)	Re_{∞}	D = 1cm		D = 2 cm		D = 3 cm		Significant wall effect on bed expansion at d/D =
					d/D	Homogeneous	d/D	Homogeneous	d/D	Homogeneous	
1	Plastic (orange) balls	1.186	1.97	136	0.197	Yes	0.099	Yes	0.065	Yes	0.197
2	Plastic (brown) balls	1.205	2.48	240	0.248	Partially	0.124	Yes	0.082	Yes	0.248
3	Plastic (blue) balls	1.191	2.86	298	0.286	Partially	0.143	Yes	0.094	Yes	0.286
4	Cellulose Acetate (yellow)	1.294	2.43	285	0.243	Yes	0.122	Yes	0.080	Yes	0.243
5	Cellulose Acetate (black)	1.282	3.01	410	0.301	Partially	0.151	Yes	0.099	Yes	0.301
6	Cellulose Acetate (red)	1.287	3.48	538	0.348	No	0.174	Yes	0.114	Yes	(Slight at 0.174 and 0.114)
7	Cellulose Acetate (brown)	1.252	4.45	760	0.445	No	0.223	Yes	0.146	Yes	0.223 (slight at 0.146)
8	Cellulose Acetate (white)	1.287	4.93	971	0.493	No	0.247	Yes	0.162	Yes	0.247 (slight at 0.162)
9	Cellulose Acetate (white)	1.268	5.97	1275	0.597	No	0.299	Partially	0.196	Yes	0.299, 0.196
10	Delrin	1.389	2.38	330	0.238	Yes	0.119	Yes	0.078	Yes	0.238
11	Delrin	1.415	3.18	575	0.318	Partially	0.159	Yes	0.105	Yes	0.318
12	Delrin	1.381	3.97	788	0.397	No	0.199	Yes	0.131	Yes	(Slight at 0.199 and 0.131)
13	Delrin	1.384	4.76	1077	0.476	No	0.238	Yes	0.156	Yes	0.238 (slight at 0.156)
14	PVC	1.358	4.79	1044	0.479	No	0.240	Yes	0.157	Yes	0.240 (slight at 0.157)
15	Glass balls	2.486	1.19	205	0.119	Yes	0.060	Yes	0.039	Yes	(Slight at 0.119)
16	Glass balls	2.565	2.02	568	0.202	Yes	0.101	Yes	0.066	Yes	0.202
17	Glass balls	2.494	3.18	1150	0.318	No	0.159	Yes	0.105	Yes	(Slight at 0.159)
18	Glass balls	2.496	4.01	1700	0.401	No	0.201	Yes	0.132	Yes	(Slight at 0.201, 0.132)
19	Glass balls	2.531	4.98	2500	0.498	No	0.249	Yes	0.164	Yes	0.249 (slight at 0.164)
20	Glass balls	2.561	6.03	3375	0.603	No	0.302	Partially	0.198	Yes	0.302, 0.198
21	Glass balls	2.521	7.15	4350	0.715	No	0.358	No	0.235	Yes	0.235
22	Glass balls	2.576	8.02	5200	0.802	No	0.401	No	0.264	Yes	0.264
23	Glass balls	2.571	9.99	7700	0.999	Not attempted	0.500	No	0.328	Partially	0.328

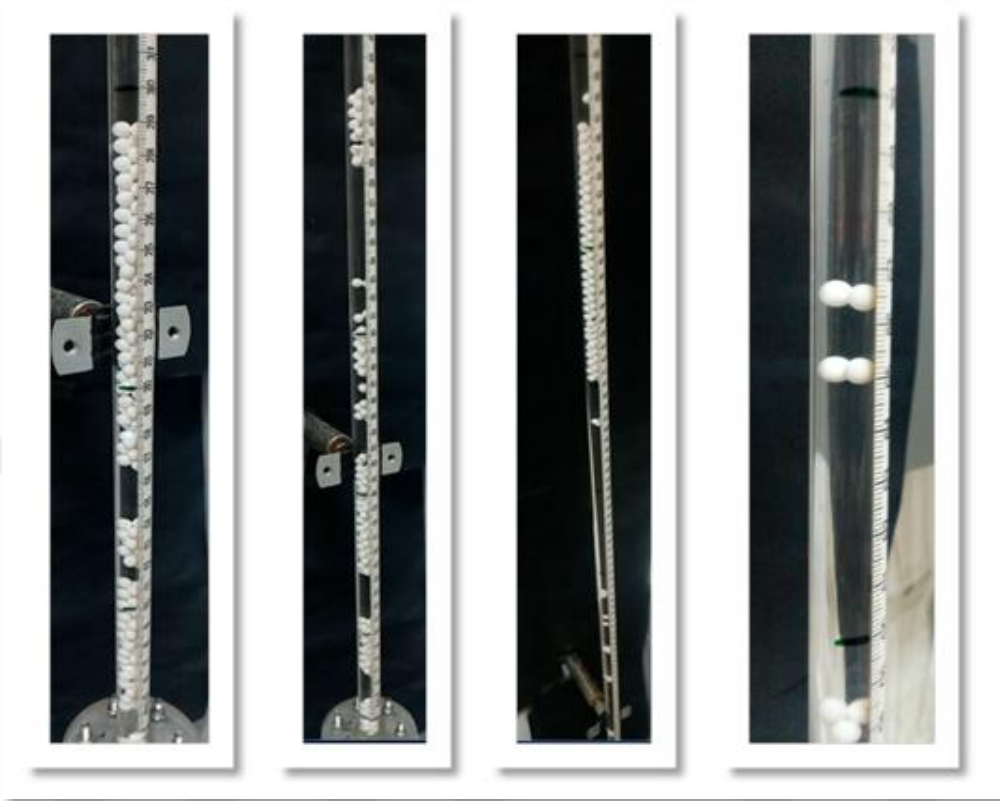


Figure 3.2 Bed fragmentation and formation of cracks in 1 cm column with 5 mm CA balls

In the rightmost picture in Figure 3.2, it is seen that formation of particle groups with 2 to 5 particles (the number depending on the d/D ratio) in the shape of a nearly horizontal ring and the movement of these groups separately from other groups and clusters.

First and second picture in Figure 3.2 and third picture in Figure 3.3 shows that the fragmentation of the bed into two or more particle clusters with large void spaces (cracks or gaps) between the clusters. These gaps were not instantaneous and the clusters tended to remain separated with large gaps between them for long periods of time.

In Figure 3.3, first picture belongs to 1 cm column with 3.5 mm CA balls, second picture belongs to 2 cm column with 8 mm glass balls, and third picture belongs to 2 cm column with 10 mm glass balls.



Figure 3.3 Bed fragmentation and formation of cracks

It is seen that lifting of the bed as a whole, leaving a large void space between the column bottom and the bottom of the lifted particle bed in the second picture in Figure 3.3.

It was occasionally possible to temporarily dispel or reduce the non-homogeneity in a fluidized bed by means of vigorous tapping of the column, but the gaps and cracks and separated particle groups re-formed quickly. Such temporarily homogenized beds were not stable or bed heights were not reproducible enough to record measurements. These experiments were therefore excluded from the analysis of wall effects on the expansion of homogeneously fluidized beds (and are indicated by the flag “No” under the column titled “Homogeneous” in Table 3.4).

In a few cases (all of which are in the range $d/D \approx 0.25$ to 0.33), Table 3.4 includes the flag “Partially” under the column titled “Homogeneous.” In these cases, fluidization tests were started with the highest expansions and the flow rate was decreased in a stepwise manner.

The bed was homogeneous at high expansions/rates but non-homogeneities of a fourth type were observed at lower rates: As the velocity was decreased to values close to the minimum fluidization velocity, the bottom of the bed settled to form a fixed-bed section which remained motionless whereas the upper part of the bed remained fluidized. Normally there were no large gaps or cracks between the two sections in such cases and the bed would look homogeneous from a distance. When the experiment was continued for a few additional minutes without changing the flow rate and without any tapping, the upper section also settled down and the entire bed looked like a fixed-bed. In these cases, it was observed that it was possible to achieve homogeneous fluidization if the column was tapped continuously. When the column was tapped in this manner, one of two things happened: (i) It was possible to keep the bed in a homogeneous state (with all parts of the bed in motion) long enough to record flow rate and bed height in a reproducible fashion and a complete bed height versus velocity curve could be generated, (ii) The bed could not made homogeneous at all or could not be kept in a homogeneous state long enough to make reliable measurements (at the low rates in question).

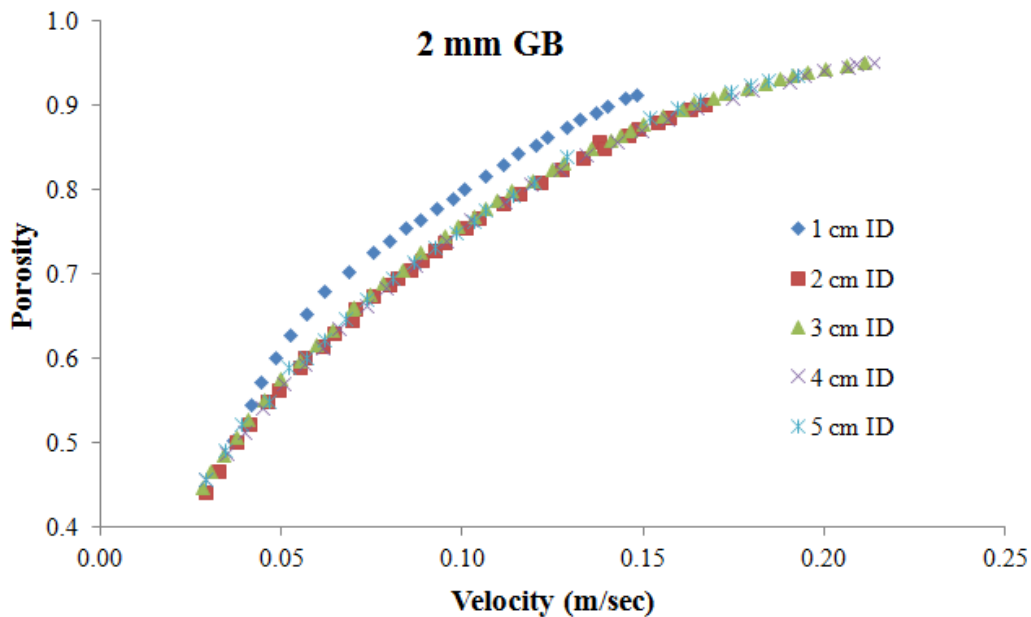


Figure 3.4 Experimental porosity values for 2 mm glass balls in 5 columns

The bed depth versus velocity measurements for the latter case were “discarded,” i.e. not included in plots such as those in Figure 3.4 and Figure 3.5 and not employed in the analysis of wall effects on bed expansion. Only a partial bed expansion versus velocity curve (i.e. data at high expansions) would then be available in such a case.

Experimental porosity values for 2 mm glass balls in 5 columns are displayed in Figure 3.4. It was possible to fluidize this bed homogeneously in all 5 columns (see Table 3.4). As a result, five different sets of expansion data –one for each column- are displayed in this figure. It is seen that the porosity observed in the 1 cm column was significantly higher than the porosities in the four larger columns for a given velocity. There is little difference between the porosity curves obtained with the four larger columns. Put in other words, the effect of wall on bed expansion was insignificant for 2cm and larger columns (i.e. for $d/D < 0.1$).

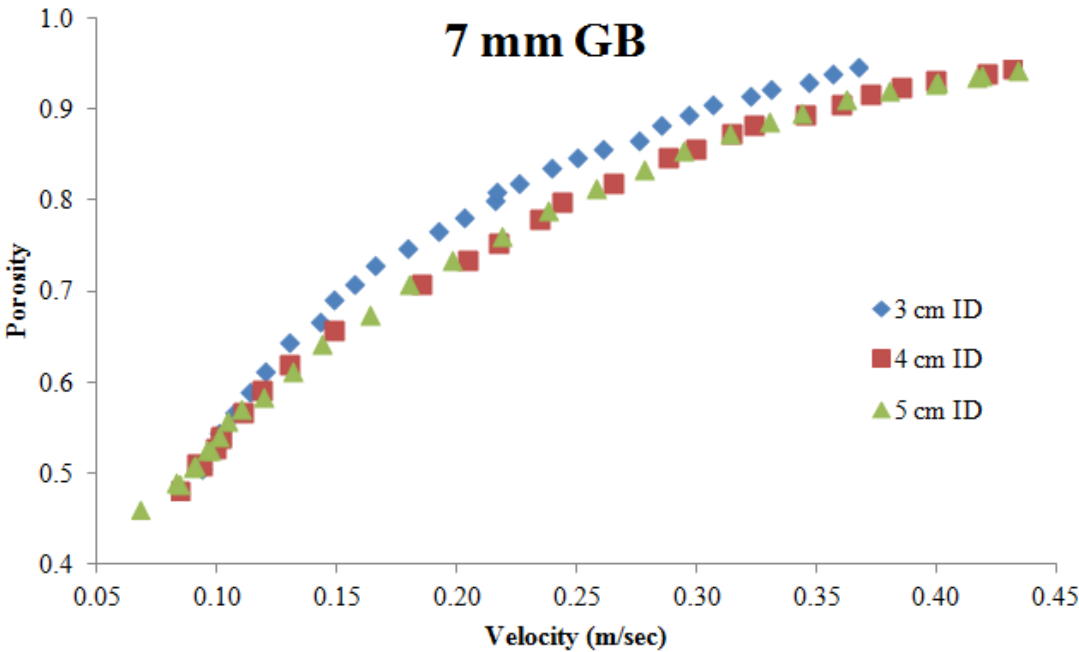


Figure 3.5 Experimental porosity values for 7 mm glass balls in 3 columns

Porosity values for 7 mm glass balls in 3 columns (diameters 3 cm, 4 cm, and 5 cm) can be seen in Figure 3.5. Homogeneous fluidization could not be achieved in 1 cm and 2 cm ID

columns with these spheres (cf. Table 3.4). Wall effect on bed expansion is seen to be significant for the 3 cm column ($d/D = 0.235$) whereas there was no noticeable difference between the porosity values observed in the 4 cm ($d/D = 0.18$) and 5 cm ($d/D = 0.14$) columns. In both Figure 3.4 and Figure 3.5, it is seen that the porosity curve for the smallest column approaches the curves for the larger columns as the velocity decreases towards the minimum fluidization velocity. The other graphs shows the porosity values are given in Appendix.

It is seen from Table 3.4 and the above discussion that homogeneous fluidization was achieved in all the experiments (a total of 91 different particle-column combinations) with $d/D < 0.25$ without any external intervention. Homogeneous fluidization could not be achieved in those experiments (16 particle-column combinations) with $d/D > 0.33$. In a total of 7 experiments with $0.25 < d/D < 0.33$, homogeneous fluidization was made possible only by tapping of the column in question over part or all of the velocity range tested. In one case (3.18 mm glass balls in the 1 cm column, i.e. $d/D = 0.318$) homogeneous fluidization did not occur even with tapping. With 3.18 mm delrin balls in the 1 cm column, on the other hand, the bed was fluidized homogeneously with some tapping of the column. The d/D values in these two cases are exactly the same, the only difference is in the densities (and, therefore, in the $Re_{t\infty}$ values) of the two materials (Table 3.4). It is clear that the ratio d/D affects the presence or absence of non-homogeneities in fluidized beds; if a second factor (such as $Re_{t\infty}$) is significant or not cannot be deduced from the present data. Generating data with different fluids using the same particle-column combinations (so that several different $Re_{t\infty}$ values can be tested for each d/D value) could be helpful to clarify this point.

The last column in Table 3.4 summarizes the observations for all the 23 spheres used in the tests. Only in two cases, namely for ~6mm CA and ~6mm glass balls, significant wall effect on bed expansion was observed with two column diameters instead of only with the smallest column. In both of these two cases, the d/D values were approximately 0.3 and 0.2. In both cases, the wall effect was more pronounced with the larger d/D value i.e. with $d/D=0.3$. In five cases (3.5 mm CA, 4 mm delrin, 1 mm, 3 mm and 4 mm glass balls), the

observed wall effects were termed “slight” as the porosity curves for the smallest columns were not significantly above those obtained in the largest columns. In five cases, there was a significant wall effect with the smallest column, with a slight effect with the next smallest column (cf. the rightmost column in Table 3.4).

An inspection of the last column in Table 3.4 reveals the following general observations: There was a significant wall effect on bed expansion for $d/D > 0.2$, whereas slight effects were observed for $0.11 < d/D < 0.2$, and the effect on bed expansion was negligible for $d/D < 0.11$. In considering these results, it should be remembered that water was used as the fluidization medium in the present work, and despite the large number of different particles used in the tests, the particle Reynolds number is restricted to values larger than 100. More importantly, a wide range $Re_{t\infty}$ values could not be obtained for fixed d/D values. This can be achieved by using different fluids with the same particles and equipment.

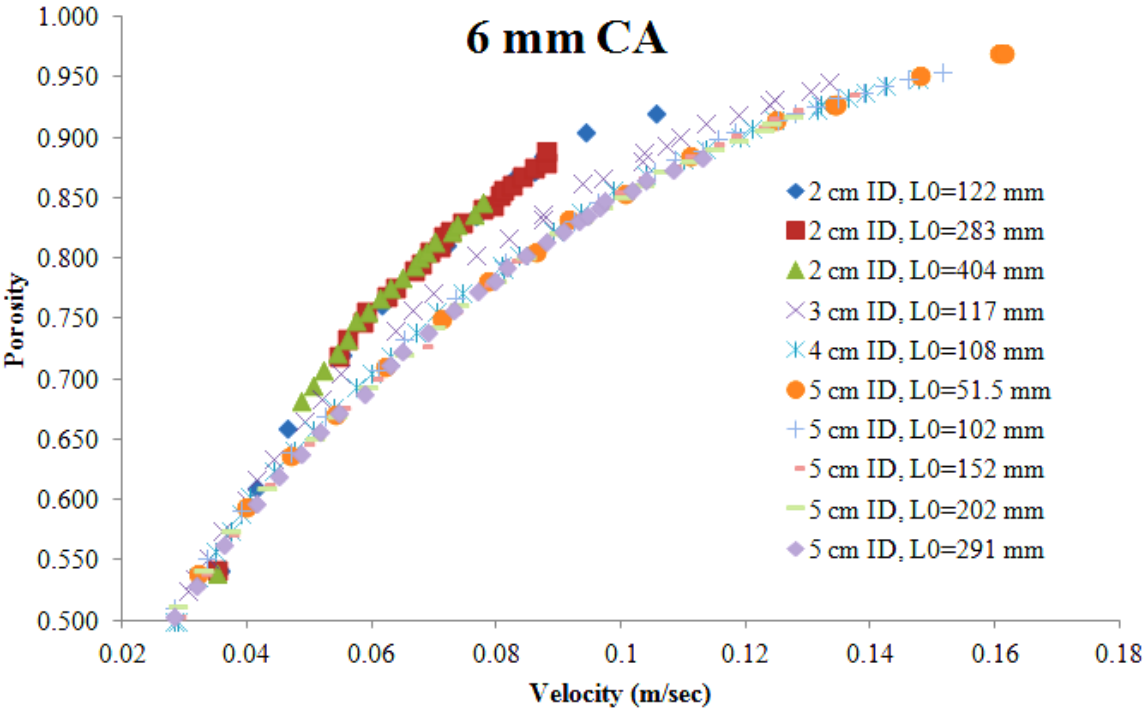


Figure 3.6 Porosity graph of 6 mm CA

Other noteworthy graphs are Figure 3.6, Figure 3.7, Figure 3.8. An example for the effect of initial bed height was showed in Figure 2.6 before. Likewise, in Figure 3.6 different values of initial bed heights were examined not only in one column but also in a second column for the same material which was 6 mm CA. This graph also shows that highest expansion of the bed can be seen with the initial bed height of 5.15 cm in the 5 cm ID.

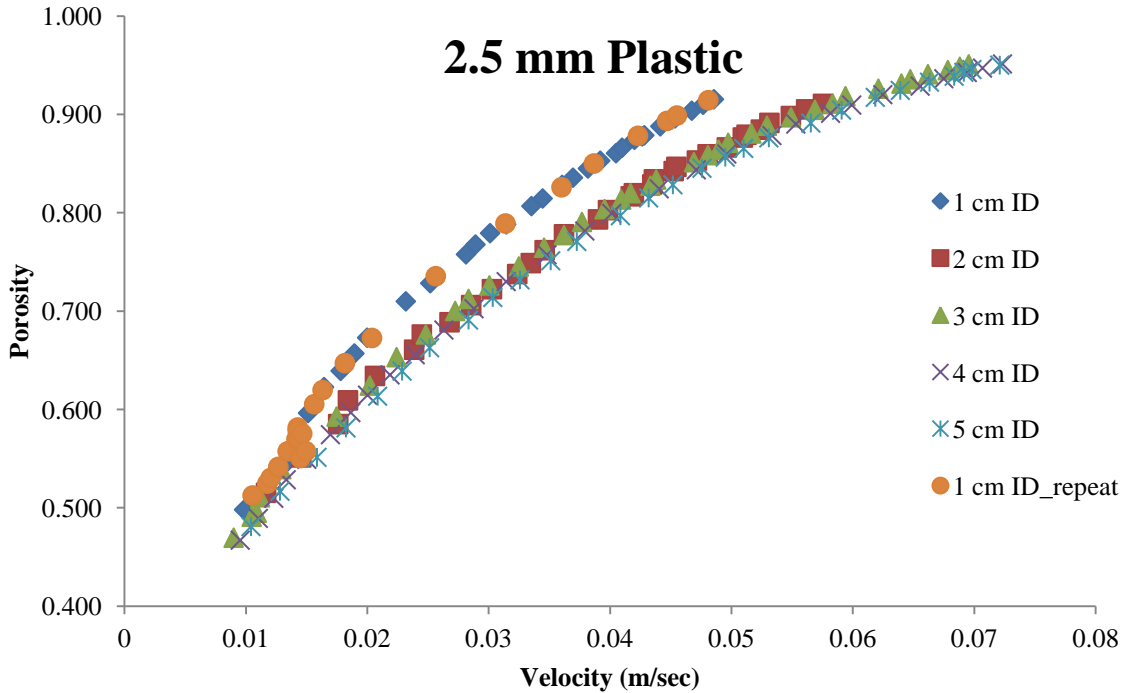


Figure 3.7 Porosity graph of 2.5 mm Plastic

Significant wall effect is seen in Figure 3.7, and Figure 3.8 for column of 1 cm ID. Another important observation here is that a different trend was followed below porosity values of 0.6 in the same column. This is why these experiments were indicated by the flag “partially” in Table 3.4. Because data below the porosity value of 0.6 was obtained with tapping to the column. The experiment results did not change even if the experiment was repeated.

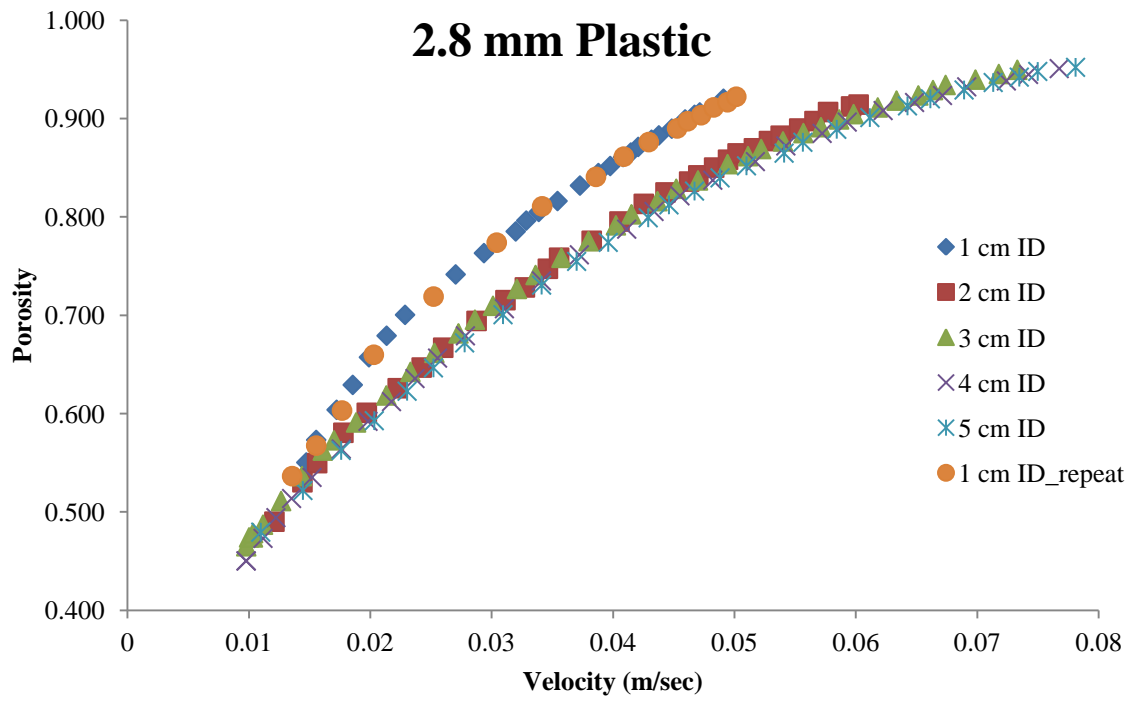


Figure 3.8 Porosity graph of 2.8 mm Plastic

4 CONCLUSIONS

Fluidization experiments were carried out with 23 different spheres in 5 columns with different diameters. The main goal of this work was the evaluation of the effects of column size on bed expansion during fluidization. Apart from its possible effects on bed expansion, however, it was observed that column size has a very significant impact on the quality of fluidization. Extreme non-homogeneities were observed for high values of d/D , while these non-homogeneities disappeared in larger columns. The findings of this study can be summarized as follows:

- For the spherical particles used in the present study, homogeneous fluidization was not possible for $d/D > 0.33$.
- Homogeneous fluidization was achieved only by vigorous tapping and/or for part of the tested velocity range for $0.25 < d/D < 0.33$. For this particle to column diameter ratio range, the fluidized beds tended to be homogeneous at higher expansions, whereas non-homogeneities in the form of interlocked sectional clusters (i.e. bed sections similar to fixed-beds co-existing with fluidized sections) occurred at the lowest rates.
- While it is clear that particle to column diameter ratio has a very significant impact on the quality of fluidization, the effect of particle Reynolds number (Re_{tco}) -if any- is not clear from the data collected in this work. Experiments with other fluids are needed to clarify this point.
- Expanded bed height during homogeneous fluidization is influenced by column size when the ratio d/D is large: At a given linear velocity, the smallest column always resulted in the largest porosity.
- In general, the effect of column size on bed expansion was significant in the smallest column in which homogeneous fluidization was possible for the given particle size and decreased and became negligible quickly with decreasing d/D values. Only in two cases (with ~6 mm CA and ~6 mm glass balls), significant wall effect on bed expansion was

observed with two column diameters. In both of these two cases, the two d/D values were approximately 0.3 and 0.2.

- Wall effect on bed expansion was observed to be significant for $d/D > 0.2$, whereas slight effects were observed for $0.11 < d/D < 0.2$, and the effect on bed expansion was negligible for $d/D < 0.11$.

It is believed that a definitive analysis may be possible only after the completion of new experiments with fluids other than water to extend the $Re_{t\infty}$ range (approximately 136 to 7700) tested in this work, especially into smaller particle Reynolds numbers. The collection of additional data may then lead to the development of a general model for a quantitative prediction of wall-effects on bed expansion in liquid-solid fluidization.

REFERENCES

- Akgiray, O., & Soyer, E. (2006). An evaluation of expansion equations for fluidized solid-liquid systems. *Journal of Water Supply: Research and Technology - AQUA*, 55(7–8), 517–525. <https://doi.org/10.2166/aqua.2006.040>
- Couderc, J.P., Davidson, J.F., Clift, R., Harrison, D. (1985). *Incipient fluidization and particulate systems*. Academic Press, (Fluidization), 1–46.
- Dharmarajah, A. H. (1982). Effect of particle shape on prediction of velocity-voidage relationship in fluidized solid-liquid systems. Iowa State University, Ames, IA.
- Dharmarajah, A. H., & Cleasby, J. L. (1986). Predicting the expansion behavior of filter media. *Journal / American Water Works Association*, 78(12), 66–76.
- Di Felice, R. (1995). Hydrodynamics of liquid fluidisation. *Chemical Engineering Science*, 50(8), 1213–1245. [https://doi.org/10.1016/0009-2509\(95\)98838-6](https://doi.org/10.1016/0009-2509(95)98838-6)
- Epstein, N. (2003). Applications of liquid-solid fluidization. *International Journal of Chemical Reactor Engineering*, (1), 1–16.
- Erdim, E., Akgiray, Ö., & Demir, İ. (2015). A revisit of pressure drop- flow rate correlations for packed beds of spheres, 283, 488–504. <https://doi.org/10.1016/j.powtec.2015.06.017>
- Garside, J., & Al-Dibouni, M. R. (1977). Velocity-Voidage Relationships for Fluidization and Sedimentation in Solid-Liquid Systems. *Industrial & Engineering Chemistry Process Design and Development*, 16(2), 206–214. <https://doi.org/10.1021/i260062a008>
- Hartman M., Havlin, V., Svoboda, K., Kozan, A. P. (1989). Predicting voidage for particulate fluidization of spheres by liquids. *Chemical Engineering Science*, (44), 2770–2775.
- Hashizume, K., & Matsue, T. (1998). Effect of Wall on Void Fraction of Liquid-Fluidized Beds. *Transactions of the Japan Society of Mechanical Engineers Series B*, 63(612), 2797–2802. <https://doi.org/10.1299/kikaib.63.2797>
- Khan, a R., Richardson, J. F. (1990). Pressure Gradient and friction factor for sedimentation and fluidisation of uniform spheres in liquids. *Chemical Engineering Science*, 45, 255–265.
- Loeffler, A. L. J. (1953). *Mechanisms of Hindered Settling and Fluidization*. Iowa State Univ. of Sci. and Technol., Ames.
- Neuzil, L., Hrdina, M. (1965). Effects of Wall on the Expansion of a Fluidized Bed. *Chemical Communications*, 30, 752–768.
- Richardson, J. F., Davidson, J. F., Harrison, D. (1971). *Incipient fluidization and particulate systems*. Academic Press, (Fluidization), 25–64.
- Richardson, J. F., Meikle, R. A. (1961). *Sedimentation and fluidisation: Part III*. Chemical

Engineering Research and Design, 39.

Richardson, J. F., & Zaki, W. N. (1954). The sedimentation of a suspension of uniform spheres under conditions of viscous flow. *Chemical Engineering Science*, 3(2), 65–73. [https://doi.org/10.1016/0009-2509\(54\)85015-9](https://doi.org/10.1016/0009-2509(54)85015-9)

Rowe, P. N. (1987). A Convenient Empirical Equation for Estimation of Richardson-Zaki Exponent. *Chemical Engineering Science*, (42), 2795–2796.

Soyer, E., & Akgiray, O. (2009). A new simple equation for the prediction of filter expansion during backwashing. *Journal of Water Supply: Research and Technology - AQUA*, 58(5), 336–345. <https://doi.org/10.2166/aqua.2009.090>

Weast, R.C., Astle, M. J., Beyer, W. H. (1989). *CRC Handbook of Chemistry and Physics* (69th ed.). Florida.

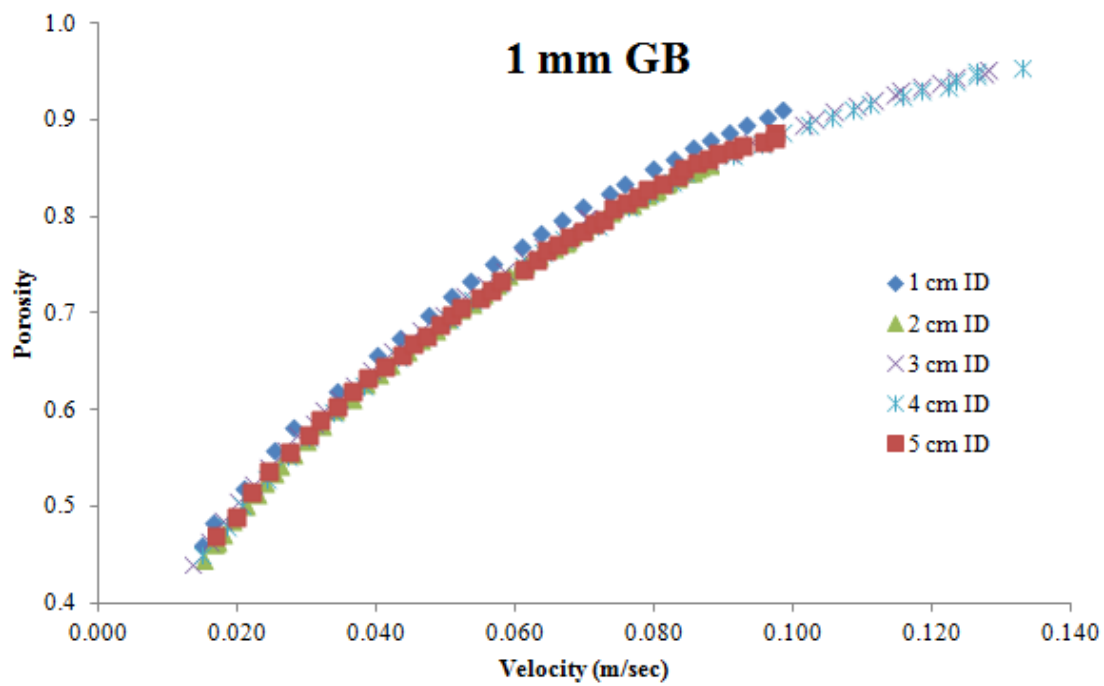
Wilhelm, R. H., Kwauk, M. (1948). Fluidization of solid particles. *Chemical Engineering Prog.*, (44), 201.

Yang, W.-C. (2003). *Handbook of Fluidization and Fluid-Particle Systems*.

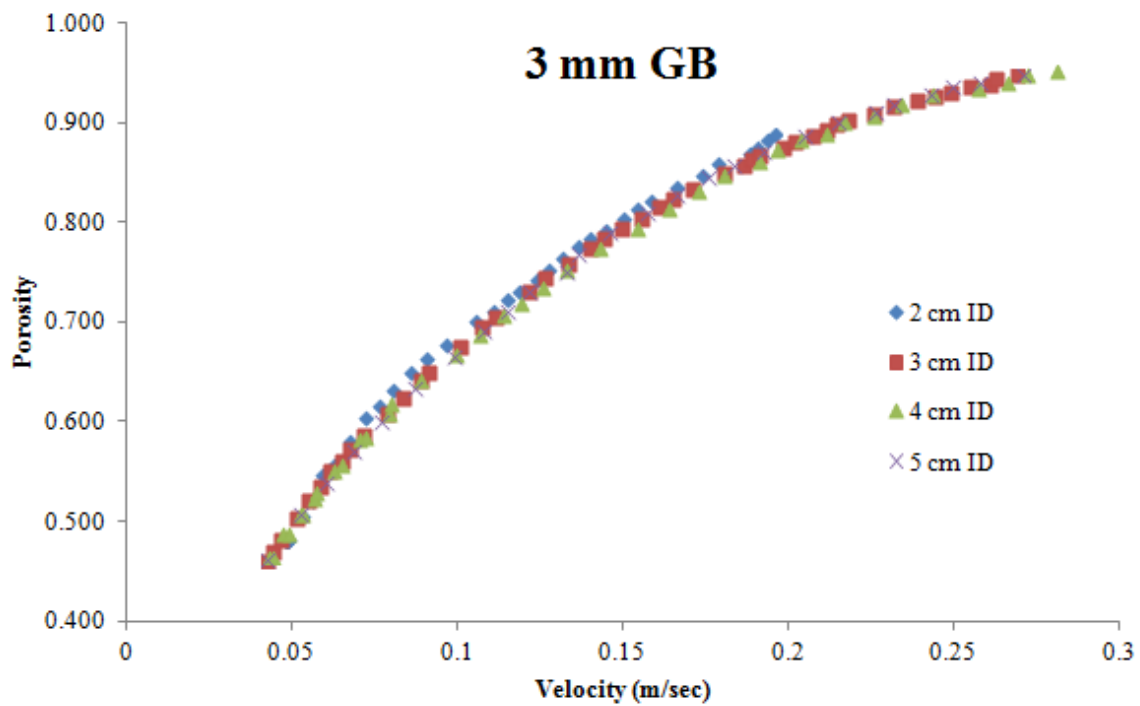


APPENDIX

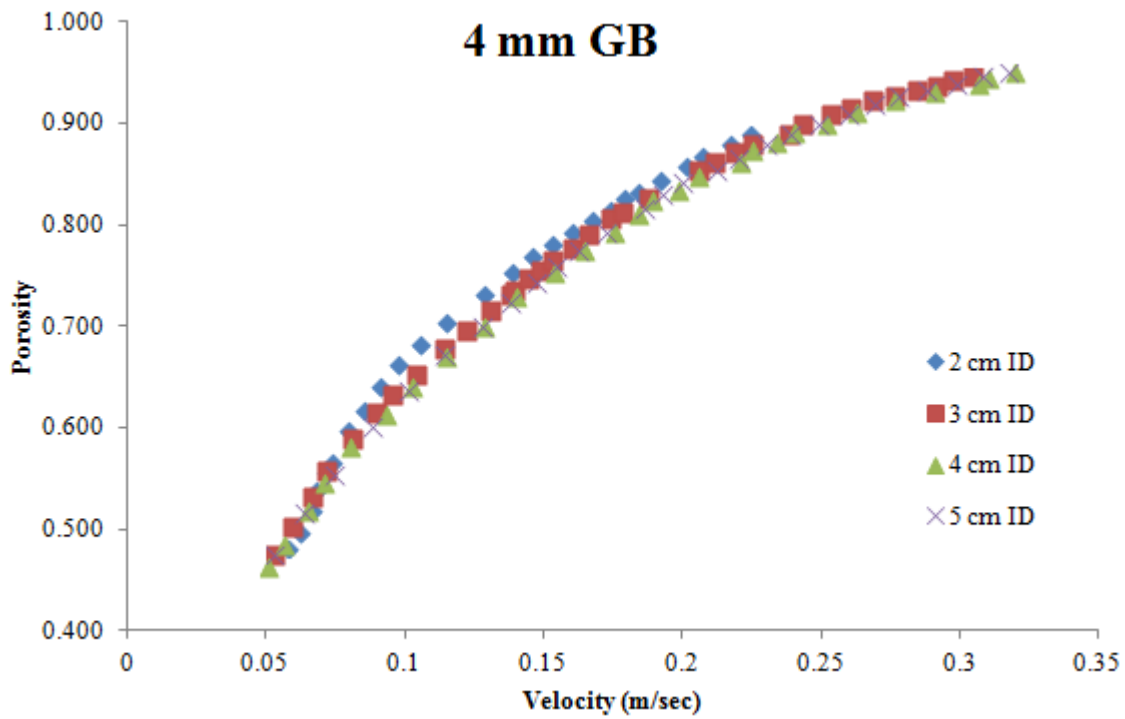
**Fluidization Graphs of
Velocity vs Porosity**



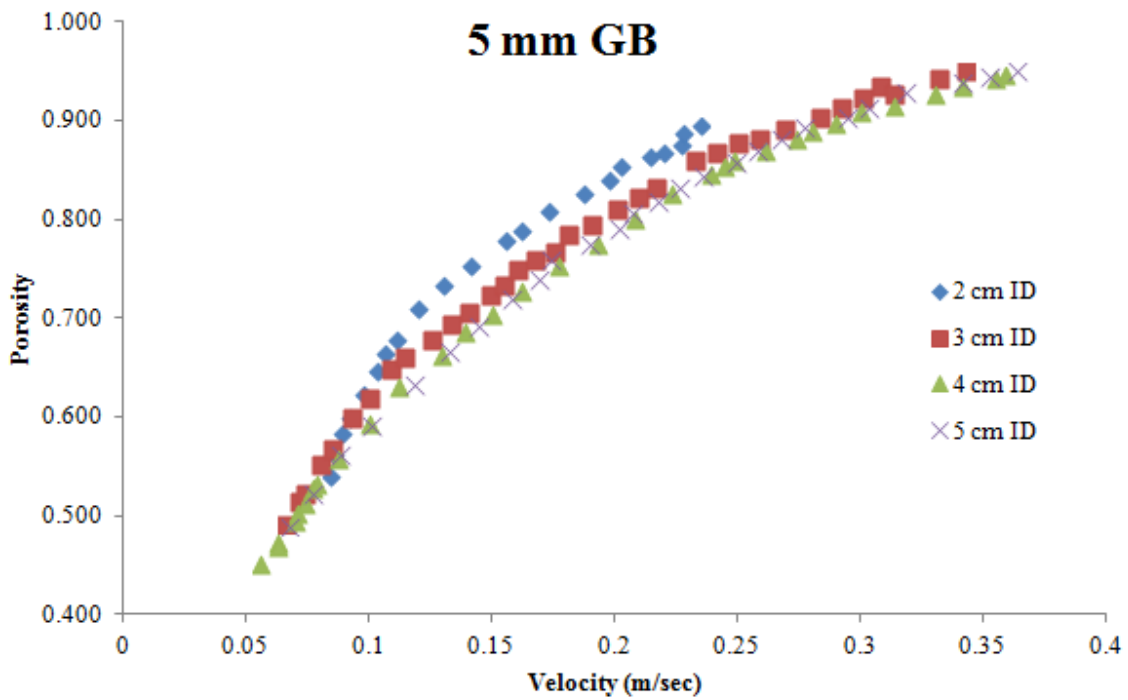
Appendix-Figure 1 Porosity graph of 1 mm GB



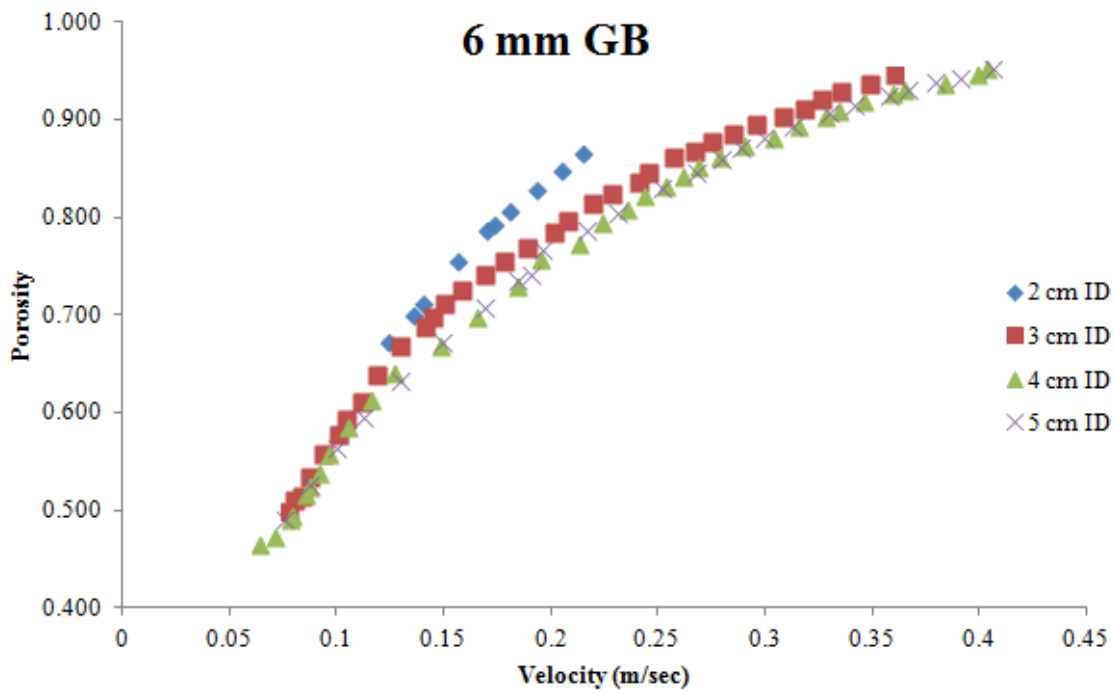
Appendix-Figure 2 Porosity graph of 3 mm GB



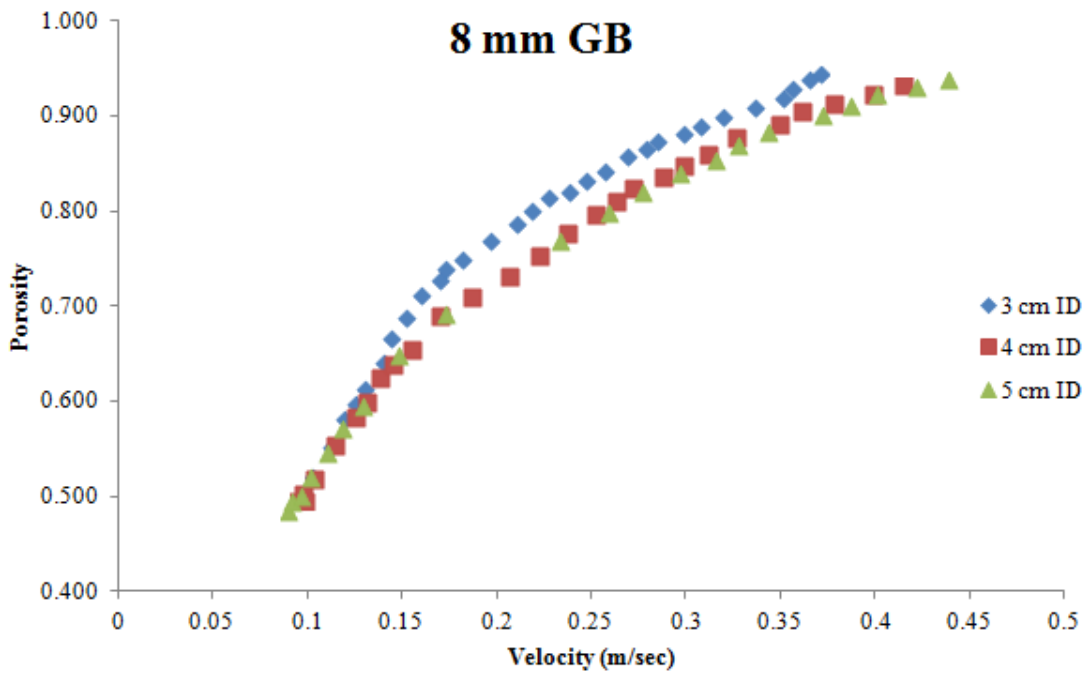
Appendix-Figure 3 Porosity graph of 4 mm GB



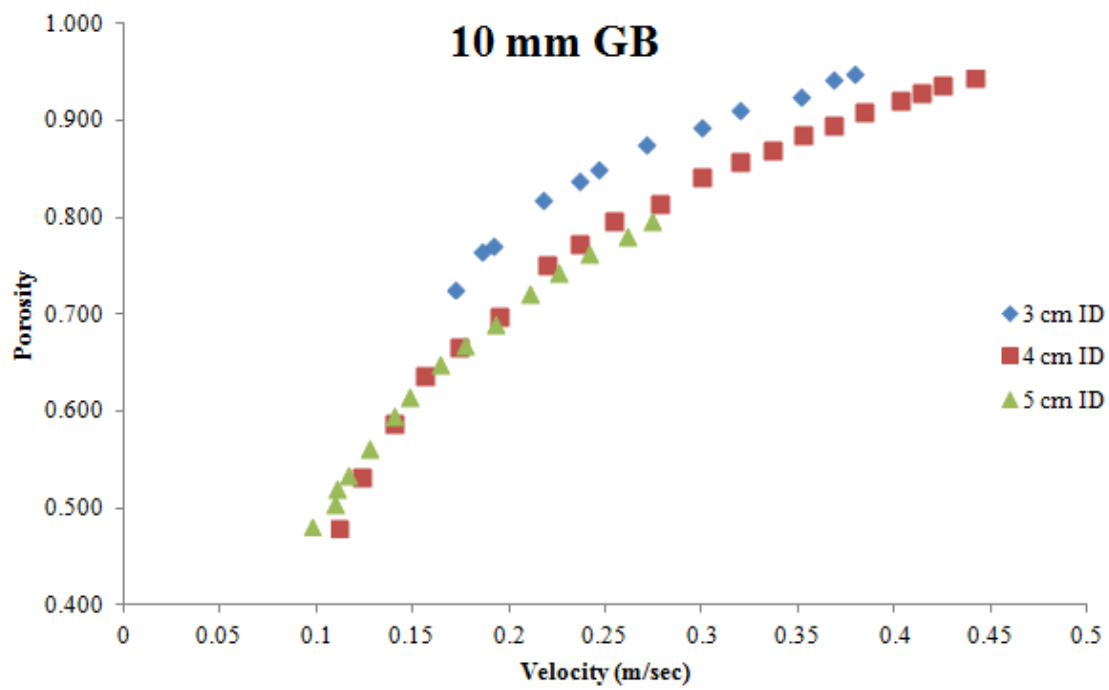
Appendix-Figure 4 Porosity graph of 5 mm GB



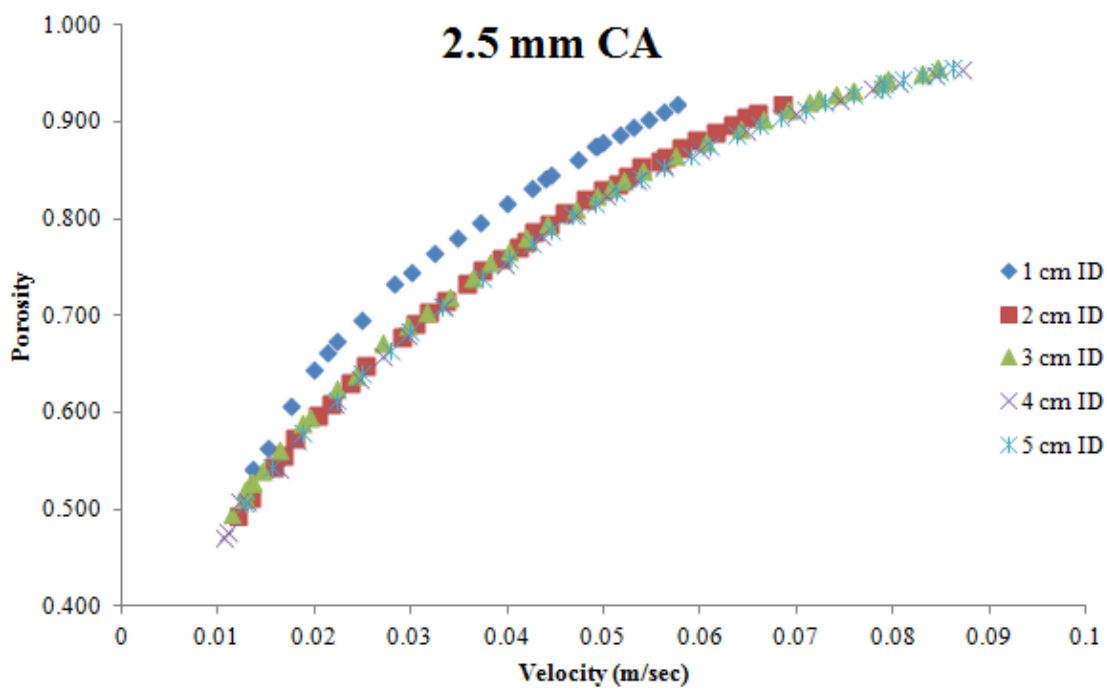
Appendix-Figure 5 Porosity graph of 6 mm GB



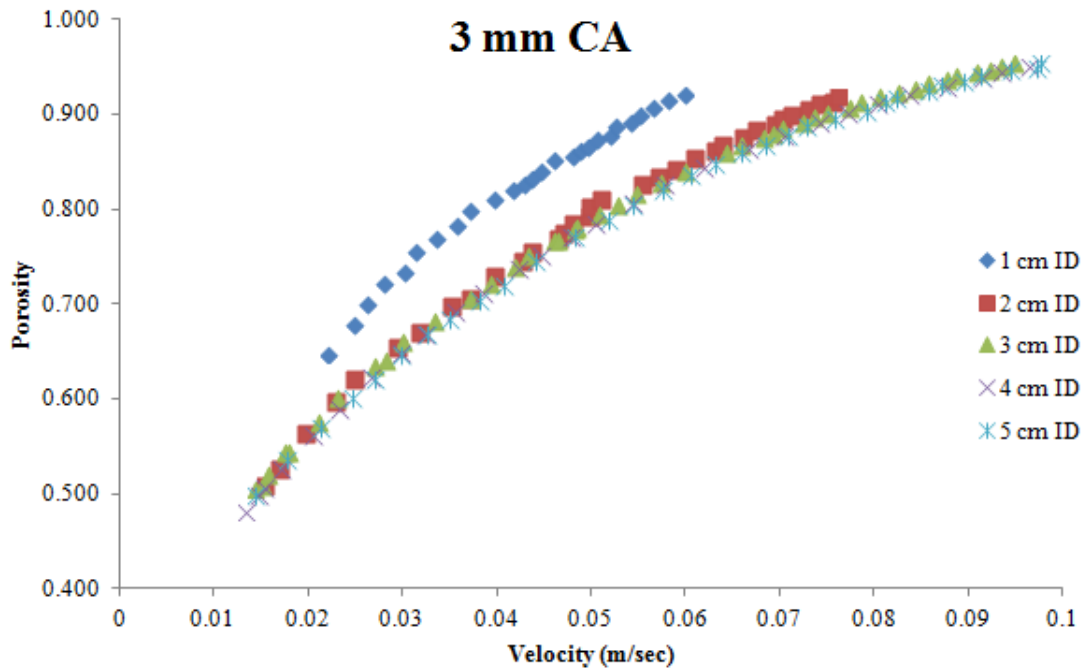
Appendix-Figure 6 Porosity graph of 8 mm GB



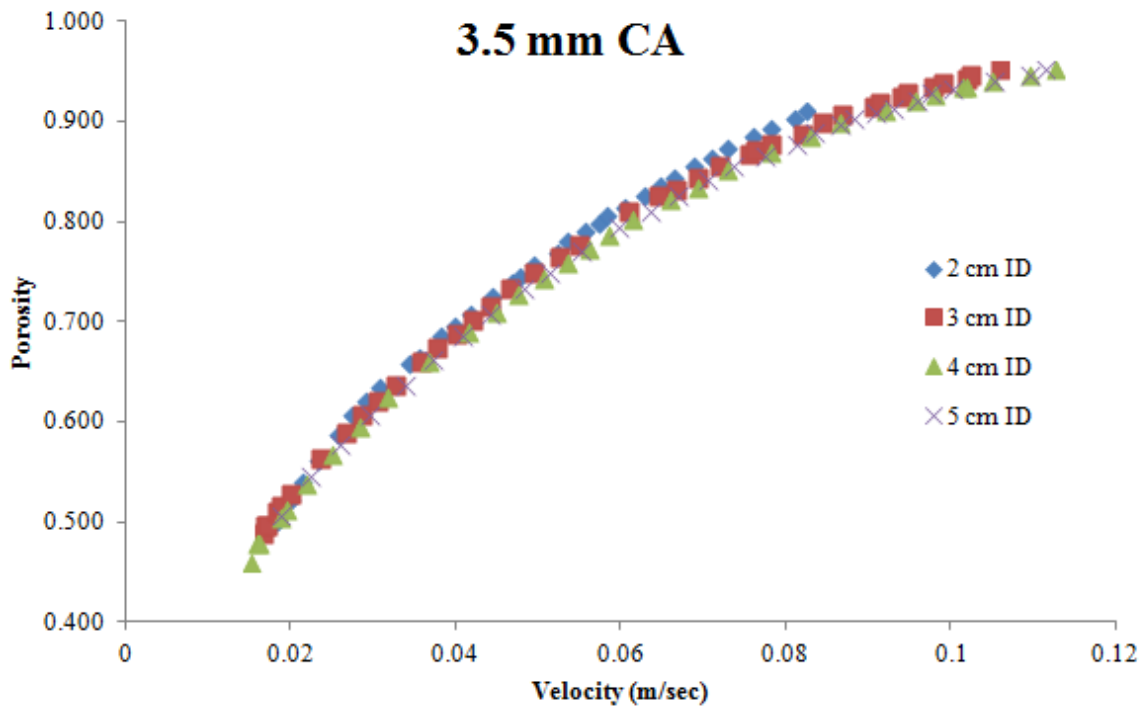
Appendix-Figure 7 Porosity graph of 10 mm GB



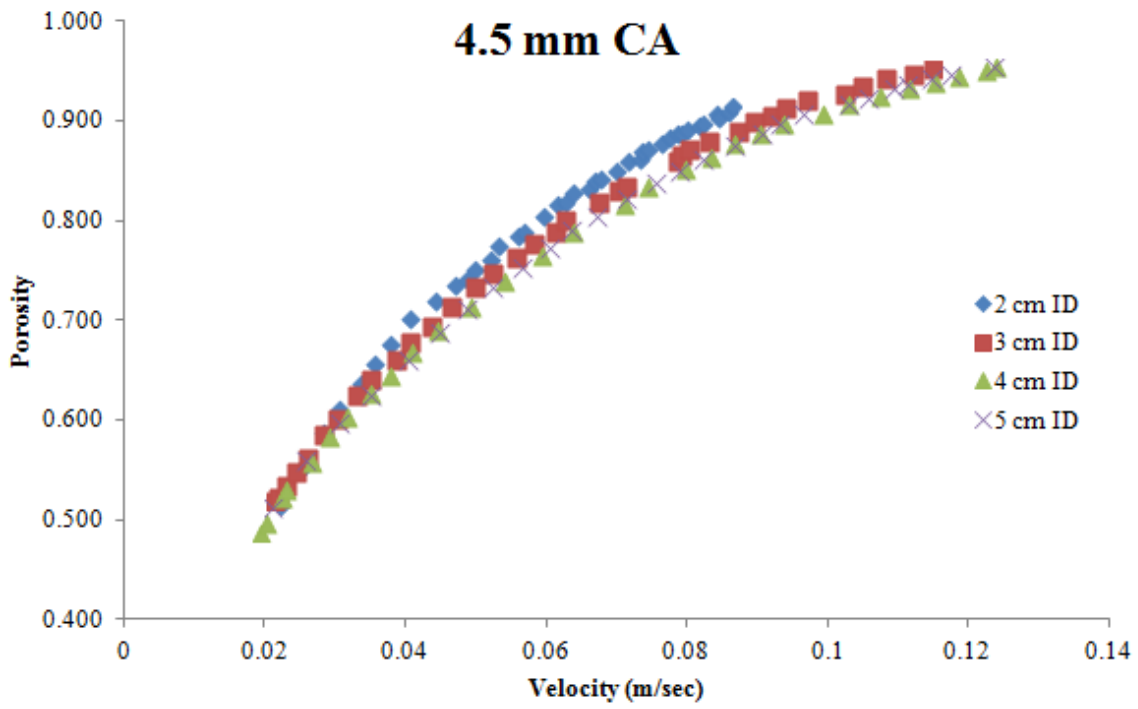
Appendix-Figure 8 Porosity graph of 2.5 mm CA



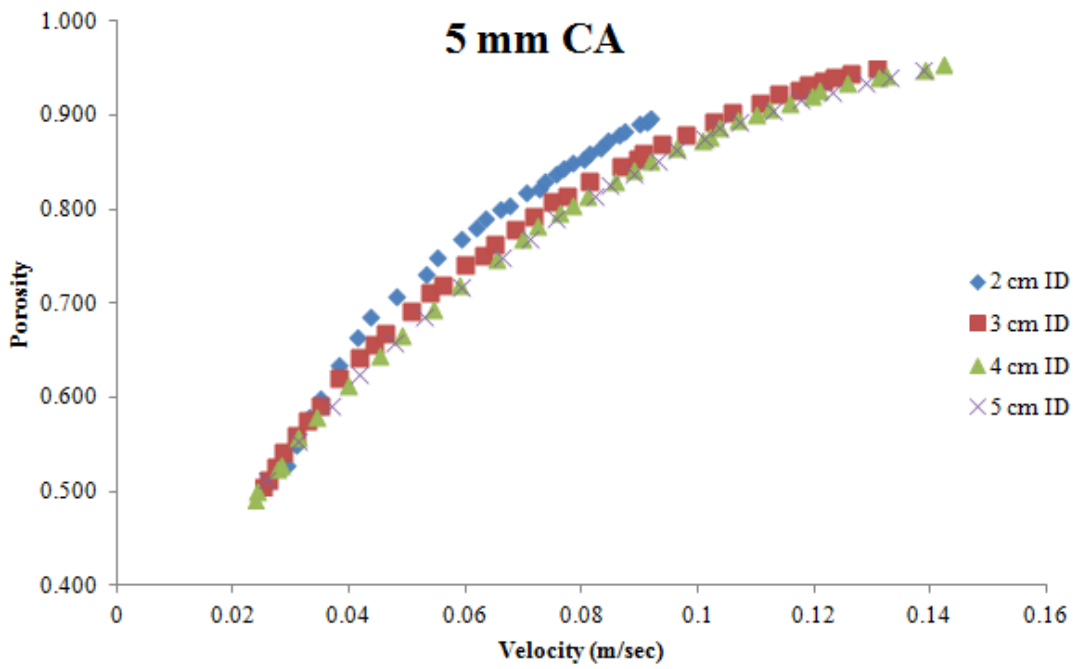
Appendix-Figure 9 Porosity graph of 3 mm CA



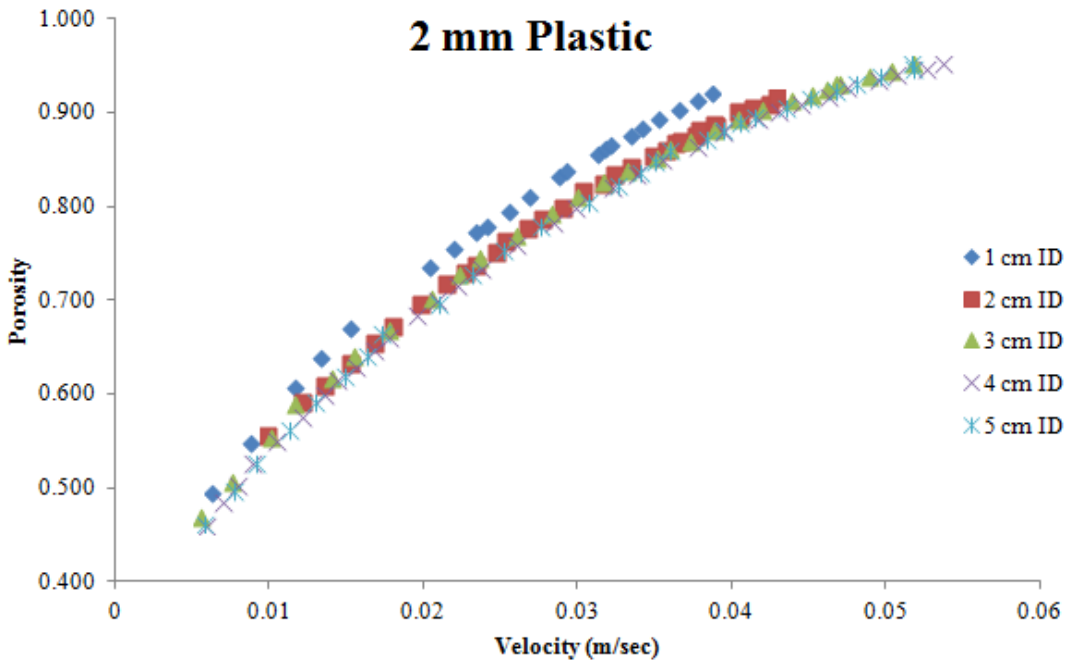
Appendix-Figure 10 Porosity graph of 3.5 mm CA



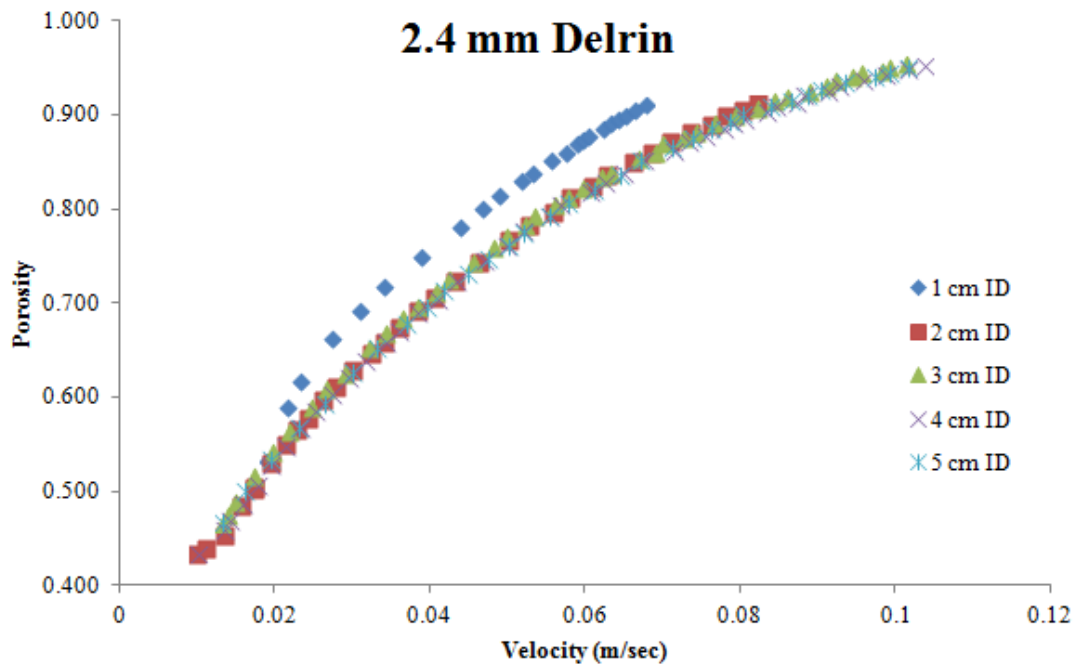
Appendix-Figure 11 Porosity graph of 4.5 mm CA



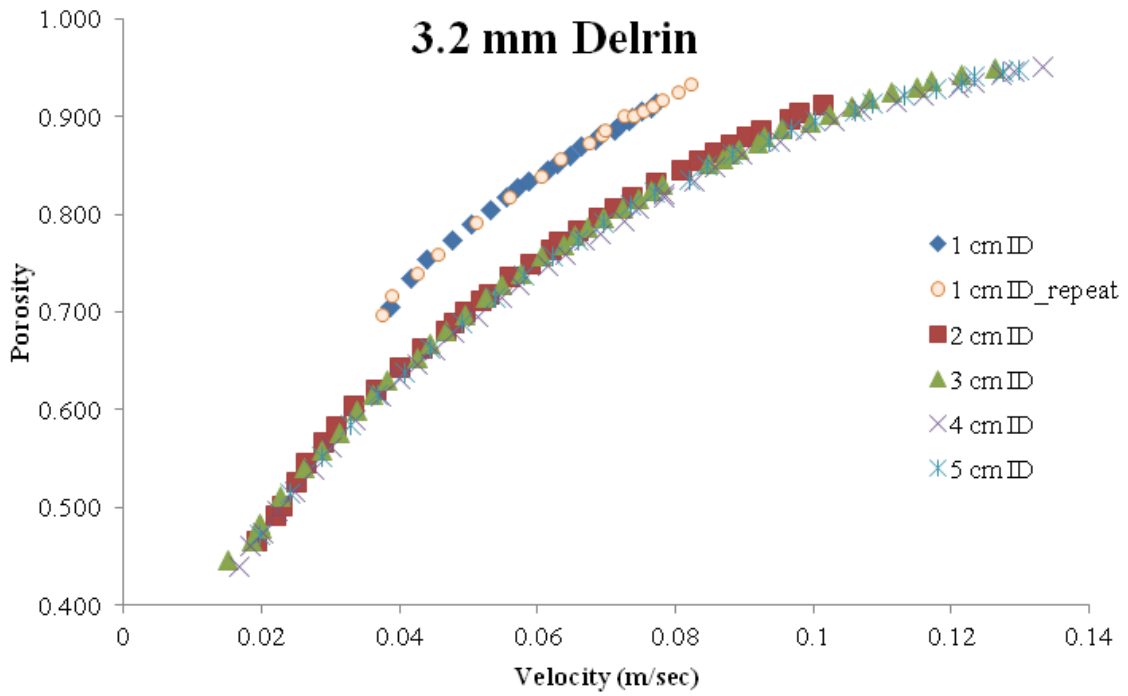
Appendix-Figure 12 Porosity graph of 5 mm CA



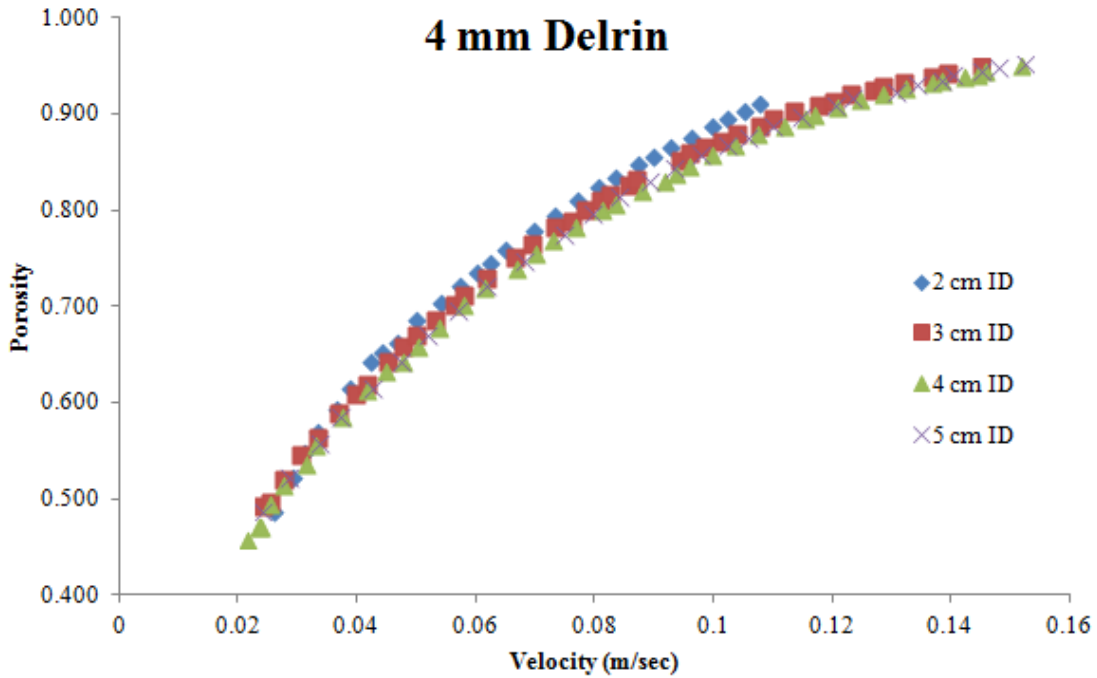
Appendix-Figure 13 Porosity graph of 2 mm Plastic



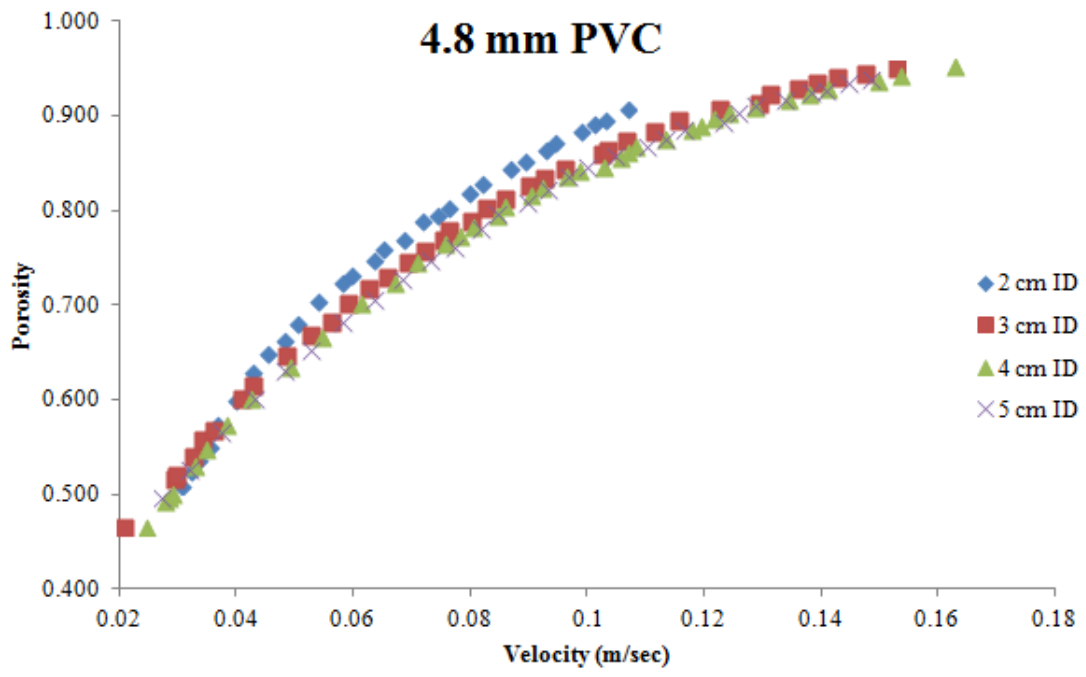
Appendix-Figure 14 Porosity graph of 2.4 mm Delrin



Appendix-Figure 15 Porosity graph of 3.2 mm Delrin



Appendix-Figure 16 Porosity graph of 4 mm Delrin



Appendix-Figure 17 Porosity graph of 4.8 mm PVC

ÖZGEÇMİŞ

1. Adı Soyadı : ÖZLEM KAPLAN

2. Doğum Tarihi : 1991

3. Öğrenim Durumu

Derece	Alan	Üniversite	Yıl
Lisans	Çevre Mühendisliği	MARMARA ÜNİVERSİTESİ	2015
Yüksek Lisans	Çevre Mühendisliği	MARMARA ÜNİVERSİTESİ	2017

4. Uluslararası Bilimsel Toplantılarda Sunulan ve Bildiri Kitabında (Proceedings) Basılan Bildiriler

Kaplan Ö., Soyer E., Akgiray Ö., “Wall Effects in Liquid-Solid Fluidization”, 2nd IWA Regional Symposium on Water, Wastewater and Environment, IWA-PPFW 2017, Çeşme-İzmir-TÜRKİYE, 22-24 Mart 2017